This is to certify that the

thesis entitled

Back Extrusion of Power Law, Bingham Plastic
and Herschel-Bulkley Fluids

presented by

Fernando Alberto Osorio-Lira

has been accepted towards fulfillment
of the requirements for

M.Sc. degree in Food Science

James F. Steffe

Major professor

James A. Steffe

Date February 19, 1985

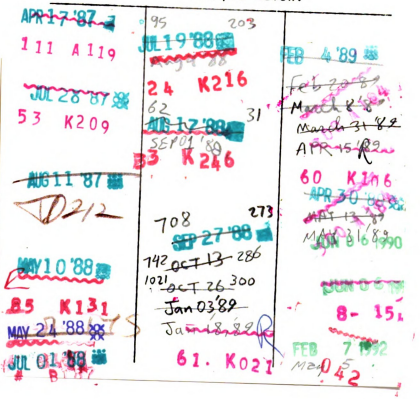

BACK EXTRUSION OF POWER LAW, BINGHAM PLASTIC AND HERSCHEL-BULKLEY FLUIDS

By

Fernando Alberto Osorio-Lira

A THESIS

Submitted to
Michigan State University
in partial fulfillment of the requirements
for the degree of

MASTER OF SCIENCE

Department of Food Science and Human Nutrition

1985

ABSTRACT

BACK EXTRUSION OF POWER LAW, BINGHAM PLASTIC AND HERSCHEL-BULKLEY FLUIDS

By

Fernando Alberto Osorio-Lira

A mathematical model was developed to describe the behavior of non-Newtonian fluids in a back extrusion device using the Herschel-Bulkley fluid model. With this mathematical model it is possible to determine the rheological properties of the fluids. The shear stress and the shear rate at the wall may also be calculated for each fluid. The mathematical expressions obtained were expressed in form of dimensionless terms; graphical aids and tables were prepared to facilitate the handling of the mathematical expressions.

The mathematical model was experimentally validated for pseudoplastic and Herschel-Bulkley fluids. Values obtained with the back extrusion device gave good results when compared with those obtained with a Haake viscometer.

Using the mathematical model developed in this study for a Herschel-Bulkley fluid in a back extrustion device, it is possible to obtain the yield stress experimentally when determining the other rheological properties of the fluid.

To: Alicia
Carolina
Pilar
Aurora
and
H. Rolando

ACKNOWLEDGMENTS

I would like to express my sincere gratitude and appreciation to Dr. James F. Steffe, my major professor, for his advice, interest and continuous support during the course of this study.

Sincere appreciation is extended to the guidance committee members: Dr. Marc Uebersax, Dr. Ajit Srivastava, and Dr. Eric Grulke.

Special thanks is extended to Marnie Laurion for the typing of this thesis.

I also express my gratitude to ODEPLAN-CHILE, for their support through a scholarship, which provided the opportunity to develop this study.

TABLE OF CONTENTS

LIST OF TABLES

LIST OF FIGURES

NOMENCLATURE

a = radius of the plunger, m

$\overline{AO}$ = level of fluid measured from the fluid surface to O, m

C_1 = constant in Equation (4), $Pa^{-1}\ s^{-1}$

C_2 = constant in Equation (4), $Pa^{-\alpha}\ s^{-1}$

C_3 = constant in Equation (5), Pa s

C_4 = constant in Equation (5), Pa^{-1}

C_5 = constant in Equation (5), s^{-1}

C_6 = constant in Equation (6), Pa

C_7 = constant in Equation (6), s^{-1}

C_{sp} = chart speed of the recorder, m/s

$\frac{dv}{dr}$ = shear rate, s^{-1}

D = diameter, m

F = force applied to the plunger, N

F_b = buoyancy force, N.

F_{cb} = force corrected for buoyancy, N

F_T = recorded force while plunger is traveling down, N

F_{T_e} = recorded force after the plunger is stopped, N

g = acceleration due to gravity, m/s^2

K = ratio of radius of plunger to that of outer cylinder, dimensionless

l_{ch} = chart length, obtained from the recorder, m

L = length of annular region = $\overline{AO} + \overline{OB}$, m

n = flow behavior index, dimensionless

O = initial level of fluid when the plunger has not been forced down in the sample, m

$\overline{OB}$ = position of the plunger bottom, measured with respect to O, m

p = static pressure, Pa

p_L = pressure in excess of hydrostatic pressure at the plunger base, Pa

p_o = pressure at entrance to annulus, Pa

P = pressure drop per unit of length, Pa/m

Q_T = total volumetric flow rate through the annulus, m^3/s

r = radial coordinate, measured from common axis of cylinder forming annulus, m

R = radius of outer cylinder of annulus, m

s = reciprocal of n, dimensionless

t = time, s

t_f = time at the end of the test, s

T = dimensionless shear stress, defined in Equation (11)

T_o = dimensionless yield stress, defined in Equation (12)

T_w = dimensionless shear stress at the plunger wall

v_p = velocity of the plunger, m/s

V = velocity, m/s

GREEK SYMBOLS

γ = mass density of fluid, kg/m^3

γ_1 = sample density, kg/m^3

ΔP = $p_o - p_L$, Pa

ΔP_b = pressure due to the buoyancy force, Pa

η = consistency coefficient, Pa s^n

η_p = plastic viscosity, Pa s

θ = temperature, ^oC

λ = value of dimensionless radial coordinate ρ for which shear stress is zero

λ_-, λ_+ = limits of plug region in Herschel-Bulkley flow, as shown in Figure 2

μ = Newtonian viscosity, Pa s

μ_∞ = viscosity at infinite shear rate, Pa s

$\rho = \frac{r}{R}$ = dimensionless radial coordinate

τ = shear stress, Pa

τ_y = yield stress, Pa

τ_w = shear stress at the plunger wall, Pa

Φ = dimensionless flow rate defined in Equation (37)

ϕ = dimensionless velocity defined by Equation (13)

ϕ_-, ϕ_+ = dimensionless velocity outside plug flow region

ϕ_{max} = dimensionless maximum velocity in the plug flow region

ϕ_p = dimensionless velocity at the plunger wall

∇ = "del" or "nabla" operator

Chapter 1

INTRODUCTION

Non-Newtonian fluids are of great importance in the processing industry. Industries in which non-Newtonian fluids are encountered include rubber, plastics, petroleum, soap and detergents, pharmaceuticals, biological fluids, atomic energy, cement, foods, paper pulp, paint, light and heavy chemicals, fermentation processes, oil field operations, ore processing, and printing (Skelland, 1967). From the above, it is evident that an understanding of non-Newtonian flow may enable a substantial economic improvement to be made in a wide diversity of processing techniques. When designing heating, cooling or pumping systems or controlling the manufacturing process for fluid foods, it is necessary to know the rheological properties of the fluid.

Instruments used to determine rheological properties, that are useful from an engineering standpoint, are those that determine relationship between shear stress and shear rate. The most used types of viscometers are the capillary tube or extrusion rheometer, the concentric cylinder rotary viscometer, the rotating cylinder in an "infinite" medium, and the cone-and-plate type of rotary viscometer (Skelland, 1967).

The fact that the Instron Universal Testing Machine (Instron Corporation, Canton, Massachusetts) is widely used in the food industry has motivated the use of a back-

extrusion device to determine rheological properties. Back-extrusion devices have been used to characterize relative flow properties of food materials; some of these devices have been designed and calibrated to measure Newtonian viscosities and others to measure subjective parameters such as gel strength (Morgan et al., 1979).

To determine flow properties with the back-extrusion technique, a sample is placed in a vertical cylinder and a plunger is forced down into the sample at a constant velocity. This causes the sample to flow upward through the annulus between the plunger and the wall of the cylinder. The force applied on the plunger is recorded as a function of time.

To date, analytical expressions to obtain rheological properties of non-Newtonian fluids in a back-extrusion device have not been available. Therefore, the objectives of this study were: 1) to develop expressions, using the Herschel-Bulkley fluid model, to describe the behavior of non-Newtonian fluids in a back-extrusion device; 2) to develop graphical aids and tables to determine the rheological properties of non-Newtonian fluids from back-extrusion data; 3) to experimentally validate the mathematical model.

Chapter 2

LITERATURE REVIEW

Non-Newtonian fluids are those for which the flow curve (shear stress versus shear rate) is not linear through the origin at a given temperature and pressure (Skelland, 1967). They are commonly divided into three broad groups, although, these classifications are by no means distinct or sharply defined:

1. Time-independent fluids are those for which the rate of shear at a given point is solely dependent upon the instantaneous shear stress at that point.

2. Time-dependent fluids are those for which the shear rate is a function of both the magnitude and the duration of shear and possibly of the time lapse between consecutive applications of shear stress.

3. Viscoelastic fluids are those that show partial elastic recovery upon the removal of a deforming shear stress. Such materials possess properties of both fluids and elastic solids.

Time-independent fluids, which are considered in this study, are sometimes referred to as "non-Newtonian viscous fluids" or alternatively as "purely viscous fluids" (Skelland, 1967).

A great many empirical or semi-empirical equations have been proposed to represent the flow behavior of materials. The choice of an equation for a particular application is to some extent a matter of taste (Whorlow, 1980). There can be

legitimate differences of opinion about the relative importance of (a) a close fit to experimental data; (b) the use of the smallest number of available constants; (c) mathematical simplicity leading to straight-forward analyses of different types of shear flow; and (d) the possibility of generalizing the equation, into tensor form, for use with more general types of flow. The equations that will be mentioned below are only those which have been used in axial laminar flow in a concentric annulus:

1. The Ostwald-de-Waele Model.

This model, also called the power law model, is the simplest and most generally useful two-constant model. The equation for the model can be written as

$$\tau = \eta \left(\frac{dv}{dr} \right)^n \qquad [1]$$

where

τ = shear stress, Pa

η = consistency coefficient, Pa s^n

$\frac{dv}{dr}$ = shear rate, s^{-1}

n = flow behavior index, dimensionless

The power law model has been used for shear-thickening materials, that is, materials which increase in viscosity as the shear stress increases. In this case, $n > 1$. For a power law fluid with $0 < n < 1$, the viscosity decreases as the shear rate increases. When $n = 1$ and $\eta = \mu$, this model simplifies to the Newtonian model.

2. The Bingham Plastic Model.

Although true Bingham plastic behavior is encountered somewhat rarely (Skelland, 1967), departure from the exact Bingham model is sometimes small enough for procedures based on this model to be useful in design. The model is

$$\tau = \tau_y + \eta_p \left(\frac{dv}{dr} \right) \qquad [2]$$

where

τ = shear stress, Pa

τ_y = yield stress, Pa

η_p = plastic viscosity, Pa s

$\frac{dv}{dr}$ = shear rate, s^{-1}

3. The Herschel-Bulkley Model.

Many non-Newtonian fluids are not well approximated by either the Bingham plastic or the power law model. They are, however, well represented by a combination model known variously as the yield-pseudoplastic (Hanks, 1979), generalized Bingham (Cheng, 1970, 1975), yield power law (Hanks and Ricks, 1974; Hanks, 1976), or Herschel-Bulkley model (Herschel and Bulkley, 1926). In this work, the model will be referred to as the Herschel-Bulkley model and be written as

$$\tau = \tau_y + \eta \left(\frac{dv}{dr} \right)^n \qquad [3]$$

where

τ = shear stress, Pa

τ_y = yield stress, Pa

η = consistency coefficient, Pa S^n

$\frac{dv}{dr}$ = shear rate, s^{-1}

n = flow behavior index, dimensionless

When $\tau_y = 0$, this model simplifies to the power law model; when n = 1, this model simplifies to the Bingham plastic model; and when $\tau_y = 0$, n = 1 and $\lambda = \mu$, this model simplifies to the Newtonian model.

4. The Ellis Model.

The Ellis model is written as

$$\tau = \frac{1}{C_1 + C_2 \tau^{(n-1)}} \left(\frac{dv}{dr} \right) \qquad [4]$$

where

τ = shear stress, Pa

C_1 = constant, $Pa^{-1}\ s^{-1}$

C_2 = constant, $Pa^{-\alpha}\ s^{-1}$

n = flow behavior index, dimensionless

$\frac{dv}{dr}$ = shear rate, s^{-1}

This model, with n > 1, shows Newtonian behavior at low shear stress and power law behavior at high shear stress (Whorlow, 1980).

5. The Powell-Eyring Model.

The Powell-Eyring model is written as

$$\tau = C_3 \left(\frac{dv}{dr} \right) + \frac{1}{C_4} \sin h^{-1} \left(\frac{1}{C_5} \left(\frac{dv}{dr} \right) \right) \qquad [5]$$

where

τ = shear stress, Pa

C_3 = constant, Pa s

C_4 = constant, Pa^{-1}

C_5 = constant, s^{-1}

$\frac{dv}{dr}$ = shear rate, s^{-1}

The equation of this model can accomodate both the low shear rate and the high-shear-rate Newtonian flow regions exhibited by some non-Newtonian fluid data (Russell and Christiansen, 1974).

6. The Williamson Model.

The Williamson model is written as

$$\tau_w = \frac{C_6(8V/D)}{C_7+(8V/D)} + \mu_{e\infty}\left(\frac{8V}{D}\right) \qquad [6]$$

where

τ_w = shear stress at the wall, Pa

C_6 = constant, Pa

C_7 = constant, s^{-1}

V = velocity, ms^{-1}

D = diameter, m

τ_{e_∞} = viscosity at infinite shear rate, Pa s

Only the Bingham plastic and Herschel-Bulkley models can be applied to fluids with yield stress.

In this study on back-extrusion, the following two facts are involved: (1) a plunger is forced down in a fluid, and (2) the fluid flows upward through a concentric annular space. Some authors have studied the two above

facts together as applied only to Newtonian fluids. The second fact has been studied by several authors and all of them but Bird et al. (1960) have considered the axial laminar flow in fixed concentric annuli. To date, the behavior of time-independent, non-Newtonian fluids in a back-extrusion device has not been considered. The findings of authors who have studied the two facts mentioned above together follow, then, the findings of those authors who have studied axial laminar flow in fixed concentric annulus will be discussed.

Bikerman (1948) developed equations to study the viscosity of Newtonian fluids by using a glass tube and a brass plunger. Constant weights on a platform--screwed to the top of the plunger--were used. To ensure the coaxial position of the plunger in the tube he used six "distance pins" to keep it centered, and therefore a correction factor for the resistance to penetration had to be added in his equations. Bikerman did not obtain expressions for the shear stress or the shear rate.

Smith et al. (1949) measured the mechanical properties of polymer solutions using an electromagnetic transducer--a plunger oscillating axially with a very small amplitude in a closed tube. The plunger was driven by a coil in a magnetic field. From electrical measurements on the coil, the mechanical resistance and reactance of the system were calculated by transducer relationships. Equations were developed for obtaining the dynamic viscosity and rigidity

of the solution. Smith et al. (1949) did not obtain equations for shear stress or shear rate.

Harper et al. (1978) used a simple glass test tube as a sample holder and a circular stainless steel rod attached to the load cell of a Model 1122 Instron as a plunger. This device was used for determining a viscosity index for heat treated bovine plasma protein suspensions. The equation for calculating the viscosity index was similar to that developed for a concentric cylinder pumping instrument described by Philippoff (1965) and Ferry (1970). The calculated viscosity index could be used only as a relative rheological property (Morgan et al. 1979). Harpet et al. (1978) did not provide equations for determining shear rate at which the index was measured.

Morgan et al. (1979) developed mathematical expressions for describing the behavior of a Newtonian fluid in a back-extruder. The authors presented analytical expressions to calculate the shear stress and the shear rate. In addition, they validated the mathematical relationships by testing Newtonian viscosity standards.

Ashare et al. (1965) extended the analysis of a falling cylinder viscometer to non-Newtonian fluids. They assumed that the annular gap is so small that the velocity profile in the gap could be taken to be the same as that for flow in a plane gap with fixed walls. They also assumed that the falling cylinder moves downward so slowly that, in solving the fluids equations of motion, one can use the approximate

boundary condition that the fluid velocity at the falling cylinder surface is zero. Correction factors are then derived to account for each of these assumptions. Specifically, they used the power law and Ellis models to reanalyse Fredrickson's (1959) data, obtaining the best agreement with the Ellis model. End effects are neglected and it is also assumed that the falling cylinder is equipped with fins to keep it centered; however, this assumption is not taken into account in the equations.

The axial laminar flow in an annular system for a Bingham plastic model was first presented by Van Olphen (1950). He estimated the solution by introducing approximations similar to those which have been used in the case of the Buckingham-Reiner equation (Melrose et al., 1958). Laird (1957) obtained the correct solution, but he did not present his results in terms of a dimensionless expression. Fredrickson and Bird (1958) obtained the exact solution in terms of dimensionless correlations for a Bingham plastic fluid flowing in an annulus. They also gave examples of how to use their charts and tables to determine rheological properties. Paslay and Slibar (1957) also solved this problem. Melrose et al. (1958) solved the problem by using dimensionless terms (different than the terms of Fredrickson and Bird, 1958) and presented their results in the form of charts and tables.

The axial laminar flow in an annular system for a power law model was first studied by Fredrickson and Bird (1958).

They presented results obtained by using power series expansions for limited values of n (flow behavior index) applied to the arguments of certain integrals which they could not solve analytically (Hanks and Larsen, 1979). Vaughn and Bergman (1966) objected to the results obtained by Fredrickson and Bird (1958) because their experimental data did not agree with the values predicted by Fredrickson and Bird (1958). Bird (1965) corroborated the fact that the power law model did not fit the experimental values obtained by Fredrickson (1959); however, Tiu and Bhattacharyya (1974) substantiated, for the first time, the theoretical fully developed velocity profiles obtained from the solution of Fredrickson and Bird (1958) by using experimental measurements of the developing and fully developed velocity profiles for inelastic power law fluids in an annulus. They used a technique employing streak photography for measuring point velocities. The test fluids employed in the experiment were five aqueous solutions of Methocel 90-HG (hydroxypropyl-methyl-cellulose) and one dilute Separan AP-30 solution (partially hydrolyzed polyacrylamide), both from the Dow Chemical Co. Fundamental fluid properties were characterized in the form of shear stress versus shear rate on a R-16 Weissenberg cone-and-plate rheogoniometer. The above result shows that Fredrickson and Bird method gives an accurate representation of experimental data when the viscometric data are truly power law.

Hanks and Larsen (1979) presented a simple algebraic

solution for the volume rate of flow of a power law non-Newtonian fluid through a concentric annulus in laminar flow. They obtained a solution which is valid for arbitrary, non integer values of s (where s = 1/n and n is the flow behavior index). This simple expression eliminates the need for either graphical interpolation or numerical integration, as is necessary in the Fredrickson and Bird (1958) model.

The axial laminar flow in an annular system for a Herschel-Bulkley model was obtained by Hanks (1979). He presented the theory of laminar flow of such fluids in concentric annuli together with appropriate design charts and practical designs examples.

Several other fluid models have been used to study the flow of axial laminar flow for annular systems. McEachern (1966) solved the equation of motion for steady axial, laminar, isothermal flow of an Ellis model fluid in a conduit of annular cross section. The results of that investigation also demonstrate that the power law viscometric representation can be used with the solution of the annulus problem given by Fredrickson and Bird (1958). Cramer and Marchello (1969) used the extended Williamson model to numerically simulate non-Newtonian flow through annuli.

According to Hanks (1979), there are reported data for a limited range of a Powell-Eyring model fluid, which were obtained by a numerical solution of the equation of motion.

Russell and Christiansen (1974) solved numerically the equation of motion for a Powell-Eyring model fluid in annuli. They demonstrated the capability of this equation to represent data that appear to be approaching Newtonian flow in both the high and the low shear rate ranges.

Rotem (1962) applied the methods of integration developed by Rotem and Shinnar (1961) for linear flow of general non-Newtonian fluids to flow in concentric circular annuli under laminar flow conditions. According to Rotem (1962), the solutions presented should apply for any incompressible, inelastic, non-Newtonian fluid in axial motion in an annular system without restrictions on the number of rheological constant used; moreover, the solution can be extended to the case of a steady, axial motion of the boundaries. He presented particular solutions for relationships including two and three rheological constant.

Finally, Savins (1958) used the pseudoplastic generalized Newtonian liquid to study linear flow in stationary pipes and annuli.

Chapter 3

Mathematical Development of the Model

The Herschel-Bulkley model was selected for this study because the flow characteristics of a large number of industrially important materials may be described by this model. In addition, the design procedure could be simplified, if necessary, to the Newtonian, power law, or Bingham plastic model because these models are special cases of the more general Herschel-Bulkley model.

3.1 Basic Equations

A Herschel-Bulkley fluid as defined in Equation [3] can be written as

$$\tau = \tau_y + \eta \left| \frac{dv}{dr} \right|^n \qquad [7]$$

where

τ = shear stress, Pa

τ_y = yield stress, Pa

η = consistency coefficient, Pa s^n

$\frac{dv}{dr}$ = shear rate, s^{-n}

n = flow behavior index, dimensionless

The absolute value of the $\frac{dv}{dr}$ term is necessary because the shear stress associated with τ_y, η and n must be in the same direction (Laird, 1957).

Consider a plunger, traveling at a constant velocity, forced down into a Herschel Bulkley fluid in a cylindrical container. The fluid flows upward through the annular space

between the plunger and inner wall of the cylinder (Fig. 1). In the developments which follow, the following assumptions are made:

a. The density is constant;

b. The fluid is homogeneous;

c. The fluid has achieved steady state flow;

d. There is no elasticity or time-dependent behavior;

e. The flow is laminar and fully developed;

f. The cylinders are sufficiently long that end effects may be neglected;

g. The temperature is constant.

In addition, the following boundary conditions are assumed for this analysis:

a. There is no slip at the annulus walls, or $v(a) = -vp$ and $v(R) = 0$;

b. The definition of a Herschel Bulkley fluid implies a region of "plug flow" where the shear stress, τ, must reduce to zero at the boundary and inside the plug.

The equations describing the flow of a compressible, isothermal fluid are the equation of continuity (Fredrickson and Bird, 1958),

$$\frac{\partial \gamma}{\partial t} + (\nabla \cdot \gamma v) = 0 \qquad [8]$$

where

γ = mass density of fluid, kg/m^3

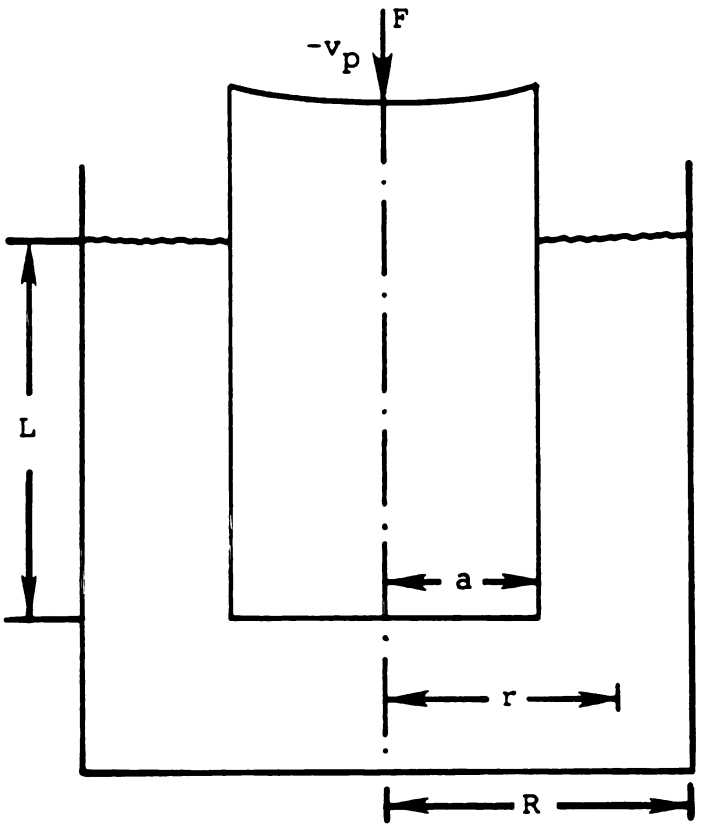

Figure 1. Schematic representation of the back-extrusion device.

v = velocity, m/s

∇ = "del" or "nabla" operator

t = time, s

and motion (Fredrickson and Bird, 1958),

$$\gamma \left[\frac{\partial v}{\partial t} + (v \cdot \nabla) v \right] = -\nabla p - (\nabla \cdot \tau) + \gamma g \qquad [9]$$

where

τ = shear stress, Pa

p = static pressure, Pa

g = acceleration due to gravity, m/s^2

For the specific system under consideration, by applying above assumptions, Equations [8] and [9] may be written in cylindrical coordinates and simplified to

$$\frac{1}{r} \frac{d}{dr} (r \tau) = \frac{p_o - p_L}{L} \qquad [10]$$

where

r = radial coordinate, m

L = length of annular region, m

p_o = pressure at entrance of annulus, Pa

p_L = pressure in excess of hydrostatic pressure at plunger base, Pa

τ = shear stress, Pa

Introducing K as the ratio of the radius of plunger to that of outer cylinder, $K = \frac{a}{R}$, and ρ as a dimensionless radial coordinate, $\frac{r}{R}$, the velocity profile for a Herschel-

Bulkley is shown in Figure 2, where λ_- and λ_+ represent the bounds on the plug flow region.

The current analysis will be conducted by introducing dimensionless variables, similar to those used by Fredrickson and Bird (1958), as

$$T = \frac{2\tau}{PR} = \text{dimensionless shear stress} \qquad [11]$$

$$T_o = \frac{2\tau_y}{PR} = \text{dimensionless yield stress} \qquad [12]$$

$$\phi = \left(\frac{2\eta}{PR^{n+1}}\right)^{1/n} \qquad v = \text{dimensionless velocity} \qquad [13]$$

$$P = \left|\frac{P_o - P_L}{L}\right| \qquad [14]$$

Note that $\frac{P_o - P_L}{L}$ is negative.

From Figure 2 it can be seen that the value of velocity increases from $\rho = K$, where $v = -v_p$, to a maximum value at $\rho = \lambda_-$; and the value of velocity decreases from $\rho = \lambda_+$ to $\rho = 1.0$ where its value is zero. The value of the $\frac{dv}{dr}$ term is positive from $\rho = K$ to $\rho = \lambda_-$ and the shear stress value, τ, is positive in this region. The value of the $\frac{dv}{dr}$ term is negative from $\rho = \lambda_+$ to $\rho = 1.0$ and the shear stress value is negative in this region.

Applying a differential force balance in the region

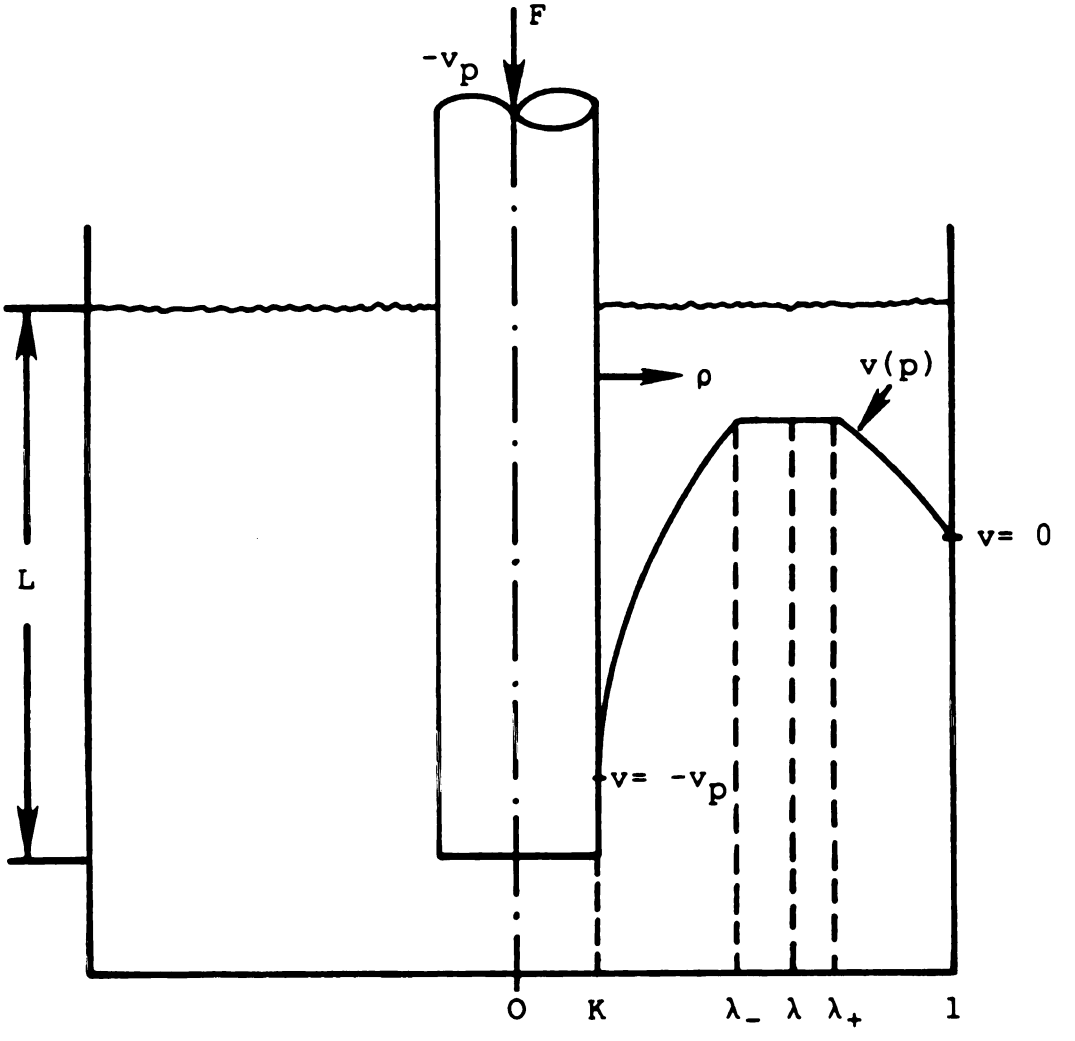

Figure 2. Schematic representation of coordinates describing axial flow in a back-extrusion device.

where $K < \rho < \lambda_-$, the acting shear force is $d(2\pi Lr\tau)$. The change in this force, as r is increased to r + dr, must equal the change in pressure force across the distance dr. Then for $K < \rho < \lambda_-$

$$d\ (2\pi Lr\tau) = d\ (\Delta P \pi r^2) \qquad [15]$$

where

$$\Delta P = p_o - p_L$$

Similarly, when $\lambda_+ < \rho < 1$ the differential force balance is

$$d\ (-2\pi Lr\tau) = d\ (\Delta P \pi r^2) \qquad [16]$$

From Equation [15]

$$d\ (2\pi Lr\tau) = d\ (\Delta P \pi r^2)$$

$$d\ (Lr\tau) = r\Delta P dr$$

and by integrating

$$\int_{r\tau}^{o} d\ (r\tau) = \frac{\Delta P}{L} \int_{r}^{\lambda R} r dr \qquad [17]$$

in which λ is the constant of integration. The radial distance $r = \lambda R$ represents the position at which $\tau = 0$.

From Equation [17]

$$-\ (r\tau) = \frac{\Delta P}{2L}\ ((\lambda R)^2 - r^2)$$

therefore,

$$\tau = \frac{\Delta P}{2L}\left(r - \frac{(\lambda R)^2}{r}\right) \qquad [18]$$

Equation [18] may also be obtained from Equation [10]. With the definition of P as

$$P = \left|\frac{\Delta P}{L}\right| = \left|\frac{P_o - P_L}{L}\right| \qquad [19]$$

one may write Equation [18] as

$$\tau = \left|\frac{\Delta P}{2L}\right|\left(\frac{(\lambda R)^2}{r} - r\right) = \frac{P}{2}\left(\frac{(\lambda R)^2}{r} - r\right) \qquad [20]$$

From Equation [16], an expression similar to Equation [20] is obtained, when $\lambda_+ < \rho < 1$, as

$$\tau = \left|\frac{\Delta P}{2L}\right|\left(r - \frac{(\lambda R)^2}{r}\right) = \frac{P}{2}\left(r - \frac{(\lambda R)^2}{r}\right) \qquad [20a]$$

Equation [20] is the starting equation for the derivation of the back extrusion model for a Herschel-Bulkley fluid.

For the Herschel-Bulkley model, the local shear stress is related to the local shear rate as

$$\tau = \pm \tau_y \pm \eta \left|\frac{dv}{dr}\right|^n \qquad [21]$$

Using the dimensionless terms defined by Equations [11] through [13] and the dimensionless radius ρ, Equation [21] may be expressed for the back-extrusion system as

$$T = \pm T_o \pm \left|\frac{d\phi}{d\rho}\right|^n \qquad [22]$$

where, from Equation [20]

$$T = \frac{\lambda^2}{\rho} - \rho \qquad [23]$$

λ_- and λ_+ represent the bounds on the plug flow region. They are those value of ρ for which $|T| = T_o$ in the region $\lambda_- < \rho < \lambda_+$; therefore,

$$+T_o = \frac{\lambda^2}{\lambda_-} - \lambda_- \qquad [24]$$

and

$$-T_o = \frac{\lambda^2}{\lambda_+} - \lambda_+ \qquad [25]$$

Then, from Equation [24]

and from Equation [25]

so the following useful relations may be obtained as

$$\lambda_- = \lambda_+ - T_o \qquad [26]$$

$$\lambda^2 = \lambda_+ (\lambda_+ - T_o) \qquad [27]$$

$$\lambda^2 = \lambda_+ \lambda_- \qquad [28]$$

It is convenient to express all the final results in terms of either λ_+ or λ_-. To follow a similar notation as used by Fredrickson and Bird (1958), the results will be expressed in terms of λ_+.

3.2 Differential Equations for the Velocity Profile

a) Region where $K < \rho < \lambda-$

The equations describing the system are, from Equations [22] and [23],

$$T = +T_o + \left(\frac{d\phi}{d\rho}\right)^n$$

and

$$T = \frac{\lambda^2}{\rho} - \rho$$

Combining these equations and rearranging yields

$$\left(\frac{d\phi}{d\rho}\right) = \left(\frac{\lambda^2}{\rho} - \rho - T_o\right)^s \qquad [29]$$

where: $s = 1/n$

b) Region where $\lambda_- < \rho < \lambda_+$

In this region

$$\left(\frac{d\phi}{d\rho}\right) = 0 \qquad [30]$$

c) Region where $\lambda_+ < \rho < 1$

The equations describing the system are

where it should be noted that T is negative in this region.

Combining both equations and rearranging yields

$$\left(-\frac{d\phi}{d\rho}\right) = \left(\rho - \frac{\lambda^2}{\rho} - T_o\right)^s \qquad [31]$$

where s = 1/n

Two methods can be used to solve the above differential equations. One is by using a binomial expansion which was the method used by Fredrickson and Bird (1958) to solve the axial laminar flow of power low fluids in concentric annuli. The problem with this solution, however, is that the values of s (defined as the inverse of the flow behavior index) have to be integer, and to use non-integer s values it is necessary to interpolate after solutions have been obtained for integer s values.

The second method, the one used in this study, makes use of the integration properties; by interchanging the order of integration and then by numerical methods it is possible to solve the problem. This was the method used by Hanks (1979) to solve the axial laminar flow of Herschel-Bulkley fluids in concentric annuli. With this method it is possible to use any value of s.

3.3 Using Integration Properties to Obtain Velocity Profile

a) Region where $K < \rho < \lambda_-$

Integrating Equation [29] yields

$$\phi_- = \int_K^{\rho} (\lambda^2 - \rho^2 - T_o\rho)^s \, \rho^{-s} \, d\rho - \phi_P \qquad [32]$$

b) Region where $\lambda_- < \rho < \lambda_+$

From Equation [29]

$$\phi_- \ (\rho = \lambda_-) \ = \ \phi_+ \ (\rho = \lambda_+) \ = \ \phi_{max} \qquad [33]$$

c) Region where $\lambda_+ < \rho < 1$

Integrating Equation [31] yields

$$\phi_+ = \int_{\rho}^{1} (\rho^2 - \lambda^2 - T_o\rho)^s \ \rho^{-s} \ d\rho \qquad [34]$$

Using Equations [32] and [34], Equation [33] may be expressed as

$$\int_{K}^{\lambda_-} (\lambda^2-\rho^2-T_o\rho)^s \ \rho^{-s} d\rho - \int_{\lambda_+}^{1} (\rho^2-\lambda^2-T_o\rho)^s \ \rho^{-s} \ d\rho = \phi_p \qquad [35]$$

3.4 Volumetric Flow Rate

The volumetric flow rate through the annulus is given by

$$Q_T = 2\pi \int_{a}^{R} v \ r \ dr \qquad [36]$$

Changing this expression to dimensionless terms yields

$$\frac{Q_T}{\pi R^3} \left(\frac{2\eta}{PR} \right)^s = \phi = 2 \int_{K}^{1} \phi\rho d\rho \qquad [37]$$

Then, introducing Equations [32], [33] and [34] in Equation [37] yields

$$\phi = 2\left\{ \int_K^{\lambda_-} \rho d\rho \int_K^{\rho} (\lambda^2-\rho^2-T_o\rho)^s \rho^{-s} d\rho - \phi_p \int_K^{\lambda_-} \rho d\rho + \right.$$

$$\left. \phi_{max} \int_{\lambda_-}^{\lambda_+} \rho d\rho + \int_{\lambda_+}^{1} \rho d\rho \int_{\rho}^{1} (\rho^2-\lambda^2-T_o\rho)^s \rho^{-s} d\rho \right\} \quad [38]$$

Interchanging the order of integration in the above expression, the following expression is obtained:

$$\phi = \left\{ 2 \int_K^{\lambda_-} (\lambda^2-\rho^2-T_o\rho)^s \rho^{-s} d\rho \int_{\rho}^{\lambda_-} \rho d\rho - \frac{\phi_p}{2} [\lambda_-^2-K^2] + \right.$$

$$\left(\int_{\lambda_+}^{1} (\rho^2-\lambda^2-T_o\rho)^s \rho^{-s} d\rho \right) \left(\frac{\lambda_+^2-\lambda_-^2}{2} \right) + \quad [39]$$

$$\left. \int_{\lambda_+}^{1} (\rho^2-\lambda^2-T_o\rho)^s \rho^{-s} d\rho \int_{\lambda_+}^{\rho} \rho d\rho \right\}$$

Integration of the $\rho d\rho$ terms and algebraic simplification gives

$$\phi = \int_K^{\lambda_-} (\lambda_-^2-\rho^2) (\lambda^2-\rho^2-T_o\rho)^s \rho^{-s} d\rho - \phi_p [\lambda_-^2-K^2] +$$

$$+ (\lambda_+^2-\lambda_-^2) \int_{\lambda_+}^{1} (\rho^2-\lambda^2-T_o\rho)^s \rho^{-s} d\rho +$$

$$+ \int_{\lambda_+}^{1} (\rho^2-\lambda_+^2) (\rho^2-\lambda^2-T_o\rho)^s \rho^{-s} d\rho$$

Expansion of terms and further simplification yields

$$\Phi = \lambda_-^2 \int_K^{\lambda_-} (\lambda^2-\rho^2-T_o\rho)\, s_\rho - s_{d\rho} - \int_K^{\lambda_-} (\lambda^2-\rho^2-T_o\rho)\, s_\rho 2 - s_{d\rho}$$
$$- \phi_\rho\, (\lambda_-^2-K^2) + \lambda_+^2 \int_{\lambda+}^1 (\rho^2-\lambda^2-T_o\rho)\, s_\rho - s_{d\rho} - \lambda_-^2 \int_{\lambda+}^1 (\rho^2-\lambda^2-T_o\rho)\, s_\rho - s_{d\rho}$$
$$+ \int_{\lambda+}^1 (\rho^2-\lambda^2-T_o\rho)\, s_\rho 2 - s_{d\rho} - \lambda_+^2 \int_{\lambda+}^1 (\rho^2-\lambda^2-T_o\rho)\, s_\rho - s\ d\rho$$

Using Equation [35] in the above expression results in

$$\Phi = \lambda_-^2\ \phi_p - \int_K^{\lambda_-} (\lambda^2-\rho^2-T_o\rho)\, s_\rho 2 - s_{d\rho} - \phi_p \lambda_-^2 + \phi_p\ K^2$$
$$+ \int_{\lambda+}^1 (\rho^2-\lambda^2-T_o\rho)\, s_\rho 2 - s_{d\rho}$$

and finally, after more simplification

$$\Phi = \phi_p K^2 - \int_K^{\lambda_-} (\lambda^2-\rho^2-T_o\rho)\, s_\rho 2 - s_{d\rho} + \int_{\lambda_+}^1 (\rho^2-\lambda^2-T_o\rho)\, s_\rho 2 - s_{d\rho} \quad [40]$$

Using this expression in Equation [37] yields

$$\Phi = \frac{Q_T}{\pi R^3}\left(\frac{2n}{PR}\right)^s = K^2\,\phi_p - \int_K^{\lambda_-} (\lambda^2-\rho^2-T_o\rho)^s \rho^{2-s} d\rho + \int_{\lambda_+}^{1} (\rho^2-\lambda^2-T_o\rho)^s \rho^{2-s} d\rho \qquad [41]$$

The volume of liquid displaced by the end of the plunger is

$$Q_T = V_p\,\pi a^2 \qquad [42]$$

and it must be equal to the volume forced up through the annulus. Therefore,

$$Q_T = \pi R^3 \left(\frac{2n}{PR}\right)^{-s} \Phi = V_p\,\pi\,a^2$$

and, by using Equation [13], with appropriate rearrangement yields

$$\Phi = \phi_p\,K^2 \qquad [43]$$

Equation [43] is solved numerically using the following calculation steps, given T_o, K and n:

1. Assume a λ_+ value.
2. With λ_+, and using Equations [26] and [27] calculate ϕ_p with Equation [35]. Calculate Φ with Equation [41].
3. With λ_+ and ϕ_p calculated in step 2, check if Equation [43] is satisfied.
4. If Equation [43] is not satisfied, return to step 1.

When Equation [43] is satisfied, the dimensionless flow rate (Φ), the limit of the plug region (λ_+) and the dimensionless velocity at the plunger wall (ϕ_p) are known. With λ_+ known, the constant of integration (λ) used in Equation [20] is obtained by using Equation [27]. It is possible to obtain the velocity profile across the annulus between the plunger wall and the inner wall of the cylinder by numerically integrating Equations [32] and [34]. The dimensionless shear stress across the annulus is calculated by placing the constant of integration into Equation [23].

Table 1 contains values of λ_+ (T_o, K, n) computed using the calculation steps described before, for a selected set of values of K and T_o for values of n from 0.1 to 1.0. Figures [3] to [12] contain values of Φ (T_o, K, n) for a selected set of values of K and T_o for values of n from 0.1 to 1.0.

3.5 Dimensionless Shear Stress at the Plunger Wall

From Equation [23], be replacing ρ by K and using Equation [27], the dimensionless shear stress at the plunger wall is found to be

$$T_w = \frac{\lambda_+(\lambda_+ - T_o)}{K} - K \qquad [44]$$

3.6 Dimensionless Shear Rate at the Plunger Wall

Replacing ρ by K in Equation [29] and using Equation [27], the dimensionless shear rate at the plunger wall is

Table 1. Values of λ_+ for different values of K, T_o and n

K = 0.1

T_o \ n	0.1	0.2	0.3	0.4	0.5	0.6	0.7	0.8	0.9	1.0
0.00	0.4065	0.4889	0.5539	0.6009	0.6344	0.6586	0.6768	0.6907	0.7017	0.7106
0.05	0.4279	0.5072	0.5707	0.6173	0.6509	0.6755	0.6939	0.7083	0.7196	0.7289
0.10	0.4508	0.5266	0.5883	0.6343	0.6678	0.6925	0.7112	0.7258	0.7374	0.7469
0.15	0.4752	0.5472	0.6068	0.6518	0.6851	0.7098	0.7286	0.7434	0.7552	0.7648
0.20	0.5012	0.5691	0.6261	0.6700	0.7027	0.7273	0.7461	0.7609	0.7728	0.7825
0.25	0.5287	0.5921	0.6464	0.6888	0.7208	0.7450	0.7637	0.7784	0.7903	0.8000
0.30	0.5578	0.6164	0.6676	0.7082	0.7393	0.7630	0.7814	0.7959	0.8077	0.8174
0.35	0.5883	0.6420	0.6898	0.7283	0.7582	0.7812	0.7992	0.8134	0.8250	0.8345
0.40	0.6202	0.6688	0.7130	0.7492	0.7776	0.7997	0.8170	0.8309	0.8421	0.8513
0.45	0.6534	0.6969	0.7371	0.7708	0.7975	0.8185	0.8350	0.8483	0.8590	0.8679
0.50	0.6879	0.7262	0.7623	0.7931	0.8178	0.8375	0.8531	0.8656	0.8758	0.8843
0.55	0.7236	0.7567	0.7886	0.8162	0.8387	0.8568	0.8713	0.8829	0.8924	0.9003
0.60	0.7604	0.7884	0.8158	0.8400	0.8601	0.8764	0.8895	0.9001	0.9088	0.9160
0.65	0.7983	0.8212	0.8441	0.8647	0.8821	0.8963	0.9078	0.9172	0.9249	0.9313
0.70	0.8370	0.8550	0.8733	0.8901	0.9045	0.9165	0.9262	0.9342	0.9407	0.9461
0.75	0.8766	0.8899	0.9036	0.9164	0.9276	0.9369	0.9447	0.9510	0.9562	0.9605
0.80	0.9171	0.9257	0.9348	0.9435	0.9511	0.9577	0.9631	0.9676	0.9713	0.9744
0.85	0.9582	0.9624	0.9669	0.9713	0.9753	0.9787	0.9816	0.9840	0.9859	0.9876

K = 0.2

0.00	0.5140	0.5680	0.6092	0.6398	0.6628	0.6803	0.6940	0.7049	0.7138	0.7211
0.05	0.5359	0.5876	0.6275	0.6577	0.6806	0.6982	0.7121	0.7232	0.7323	0.7398
0.10	0.5590	0.6081	0.6466	0.6761	0.6987	0.7163	0.7302	0.7415	0.7507	0.7584
0.15	0.5832	0.6296	0.6665	0.6951	0.7173	0.7347	0.7485	0.7598	0.7691	0.7769
0.20	0.6087	0.6521	0.6871	0.7147	0.7362	0.7533	0.7670	0.7782	0.7874	0.7952
0.25	0.6354	0.6756	0.7086	0.7348	0.7556	0.7722	0.7856	0.7966	0.8057	0.8134
0.30	0.6632	0.7001	0.7308	0.7556	0.7754	0.7914	0.8043	0.8150	0.8239	0.8314
0.35	0.6922	0.7257	0.7539	0.7770	0.7957	0.8108	0.8232	0.8334	0.8420	0.8493
0.40	0.7224	0.7522	0.7779	0.7991	0.8164	0.8306	0.8422	0.8519	0.8600	0.8669
0.45	0.7537	0.7799	0.8027	0.8218	0.8376	0.8506	0.8614	0.8704	0.8780	0.8844
0.50	0.7860	0.8085	0.8283	0.8452	0.8593	0.8710	0.8808	0.8889	0.8958	0.9017
0.55	0.8194	0.8381	0.8548	0.8693	0.8815	0.8917	0.9002	0.9074	0.9135	0.9188
0.60	0.8538	0.8686	0.8822	0.8940	0.9042	0.9127	0.9199	0.9260	0.9311	0.9356

Table 1. (continued)

T_o	0.1	0.2	0.3	0.4	0.5	0.6	0.7	0.8	0.9	1.0
0.65	0.8890	0.9001	0.9104	0.9195	0.9273	0.9340	0.9397	0.9445	0.9486	0.9521
0.70	0.9252	0.9326	0.9395	0.9456	0.9510	0.9557	0.9596	0.9630	0.9659	0.9684
0.75	0.9622	0.9659	0.9693	0.9725	0.9753	0.9777	0.9798	0.9815	0.9831	0.9844
					K = 0.3					
0.00	0.5951	0.6313	0.6587	0.6794	0.6953	0.7078	0.7177	0.7259	0.7326	0.7382
0.05	0.6175	0.6520	0.6783	0.6985	0.7142	0.7267	0.7368	0.7450	0.7519	0.7577
0.10	0.6410	0.6735	0.6986	0.7182	0.7336	0.7459	0.7559	0.7642	0.7711	0.7770
0.15	0.6655	0.6958	0.7197	0.7384	0.7534	0.7654	0.7753	0.7835	0.7904	0.7963
0.20	0.6911	0.7191	0.7414	0.7592	0.7735	0.7852	0.7948	0.8028	0.8096	0.8154
0.25	0.7176	0.7432	0.7639	0.7806	0.7941	0.8053	0.8145	0.8222	0.8288	0.8345
0.30	0.7452	0.7682	0.7871	0.8025	0.8152	0.8256	0.8343	0.8417	0.8480	0.8534
0.35	0.7738	0.7941	0.8111	0.8251	0.8367	0.8463	0.8544	0.8613	0.8676	0.8722
0.40	0.8034	0.8210	0.8358	0.8482	0.8586	0.8673	0.8746	0.8809	0.8862	0.8909
0.45	0.8339	0.8487	0.8613	0.8720	0.8810	0.8886	0.8950	0.9006	0.9053	0.9094
0.50	0.8654	0.8773	0.8876	0.8964	0.9038	0.9102	0.9156	0.9203	0.9244	0.9279
0.55	0.8977	0.9067	0.9146	0.9213	0.9272	0.9322	0.9364	0.9401	0.9433	0.9461
0.60	0.9310	0.9370	0.9423	0.9469	0.9510	0.9544	0.9574	0.9600	0.9623	0.9643
0.65	0.9651	0.9681	0.9708	0.9732	0.9752	0.9771	0.9786	0.9800	0.9812	0.9822
					K = 0.4					
0.00	0.6647	0.6887	0.7068	0.7206	0.7313	0.7399	0.7469	0.7527	0.7575	0.7616
0.05	0.6878	0.7103	0.7275	0.7409	0.7514	0.7599	0.7669	0.7727	0.7776	0.7818
0.10	0.7117	0.7327	0.7489	0.7617	0.7719	0.7803	0.7871	0.7929	0.7978	0.8020
0.15	0.7365	0.7558	0.7710	0.7830	0.7928	0.8008	0.8075	0.8132	0.8180	0.8222
0.20	0.7623	0.7798	0.7937	0.8049	0.8141	0.8217	0.8281	0.8335	0.8382	0.8425
0.25	0.7889	0.8045	0.8171	0.8274	0.8358	0.8429	0.8489	0.8540	0.8584	0.8622
0.30	0.8165	0.8301	0.8412	0.8503	0.8580	0.8644	0.8699	0.8746	0.8786	0.8822
0.35	0.8450	0.8564	0.8659	0.8739	0.8806	0.8862	0.8910	0.8952	0.8988	0.9020
0.40	0.8743	0.8836	0.8914	0.8980	0.9036	0.9083	0.9124	0.9160	0.9191	0.9218
0.45	0.9045	0.9115	0.9175	0.9226	0.9270	0.9308	0.9340	0.9368	0.9393	0.9415
0.50	0.9355	0.9402	0.9443	0.9479	0.9509	0.9535	0.9558	0.9578	0.9595	0.9611
0.55	0.9674	0.9697	0.9718	0.9737	0.9752	0.9766	0.9778	0.9788	0.9798	0.9806

Table 1. (continued)

K = 0.5

T_o	0.1	0.2	0.3	0.4	0.5	0.6	0.7	0.8	0.9	1.0
0.00	0.7280	0.7433	0.7547	0.7636	0.7705	0.7761	0.7807	0.7846	0.7878	0.7906
0.05	0.7515	0.7557	0.7765	0.7849	0.7917	0.7972	0.8017	0.8056	0.8089	0.8117
0.10	0.7759	0.7888	0.7988	0.8068	0.8132	0.8185	0.8230	0.8267	0.8300	0.8328
0.15	0.8010	0.8126	0.8218	0.8291	0.8351	0.8401	0.8444	0.8480	0.8511	0.8539
0.20	0.8270	0.8372	0.8453	0.8520	0.8575	0.8621	0.8660	0.8694	0.8723	0.8749
0.25	0.8539	0.8625	0.8695	0.8753	0.8802	0.8843	0.8878	0.8909	0.8935	0.8959
0.30	0.8815	0.8886	0.8944	0.8992	0.9033	0.9068	0.9098	0.9125	0.9147	0.9168
0.35	0.9099	0.9153	0.9198	0.9236	0.9269	0.9297	0.9321	0.9342	0.9360	0.9377
0.40	0.9392	0.9428	0.9459	0.9486	0.9508	0.9528	0.9545	0.9560	0.9573	0.9585
0.45	0.9692	0.9711	0.9727	0.9740	0.9752	0.9762	0.9771	0.9779	0.9786	0.9793

K = 0.6

0.00	0.7871	0.7962	0.8030	0.8082	0.8124	0.8158	0.8186	0.8209	0.8229	0.8246
0.05	0.8111	0.8193	0.8256	0.8305	0.8345	0.8378	0.8405	0.8429	0.8449	0.8466
0.10	0.8358	0.8431	0.8487	0.8533	0.8570	0.8601	0.8627	0.8650	0.8669	0.8686
0.15	0.8613	0.8675	0.8725	0.8765	0.8799	0.8827	0.8851	0.8872	0.8890	0.8906
0.20	0.8875	0.8927	0.8968	0.9003	0.9031	0.9056	0.9077	0.9095	0.9111	0.9125
0.25	0.9145	0.9185	0.9217	0.9245	0.9268	0.9287	0.9304	0.9319	0.9333	0.9344
0.30	0.9423	0.9450	0.9472	0.9492	0.9508	0.9522	0.9534	0.9545	0.9555	0.9563
0.35	0.9708	0.9722	0.9733	0.9743	0.9752	0.9760	0.9766	0.9772	0.9777	0.9782

K = 0.7

0.00	0.8433	0.8480	0.8516	0.8544	0.8566	0.8584	0.8599	0.8611	0.8622	0.8631
0.05	0.8676	0.8718	0.8750	0.8775	0.8796	0.8813	0.8827	0.8840	0.8850	0.8860
0.10	0.8927	0.8962	0.8989	0.9011	0.9029	0.9045	0.9058	0.9069	0.9079	0.9088
0.15	0.9185	0.9212	0.9233	0.9251	0.9267	0.9279	0.9291	0.9300	0.9309	0.9316
0.20	0.9449	0.9468	0.9484	0.9496	0.9507	0.9517	0.9525	0.9532	0.9539	0.9544
0.25	0.9721	0.9731	0.9739	0.9746	0.9752	0.9757	0.9762	0.9766	0.9769	0.9772

K = 0.8

0.00	0.8972	0.8992	0.9007	0.9019	0.9028	0.9035	0.9042	0.9047	0.9052	0.9055
0.05	0.9219	0.9235	0.9247	0.9257	0.9266	0.9273	0.9278	0.9283	0.9288	0.9292
0.10	0.9473	0.9484	0.9493	0.9501	0.9507	0.9512	0.9517	0.9521	0.9525	0.9528
0.15	0.9733	0.9739	0.9744	0.9748	0.9752	0.9755	0.9758	0.9760	0.9762	0.9764

Table 1. (continued)

K = 0.9

T_o	0.1	0.2	0.3	0.4	0.5	0.6	0.7	0.8	0.9	1.0
0.00	0.9493	0.9498	0.9502	0.9504	0.9507	0.9508	0.9510	0.9511	0.9512	0.9513
0.05	0.9744	0.9746	0.9748	0.9750	0.9752	0.9753	0.9754	0.9755	0.9756	0.9757

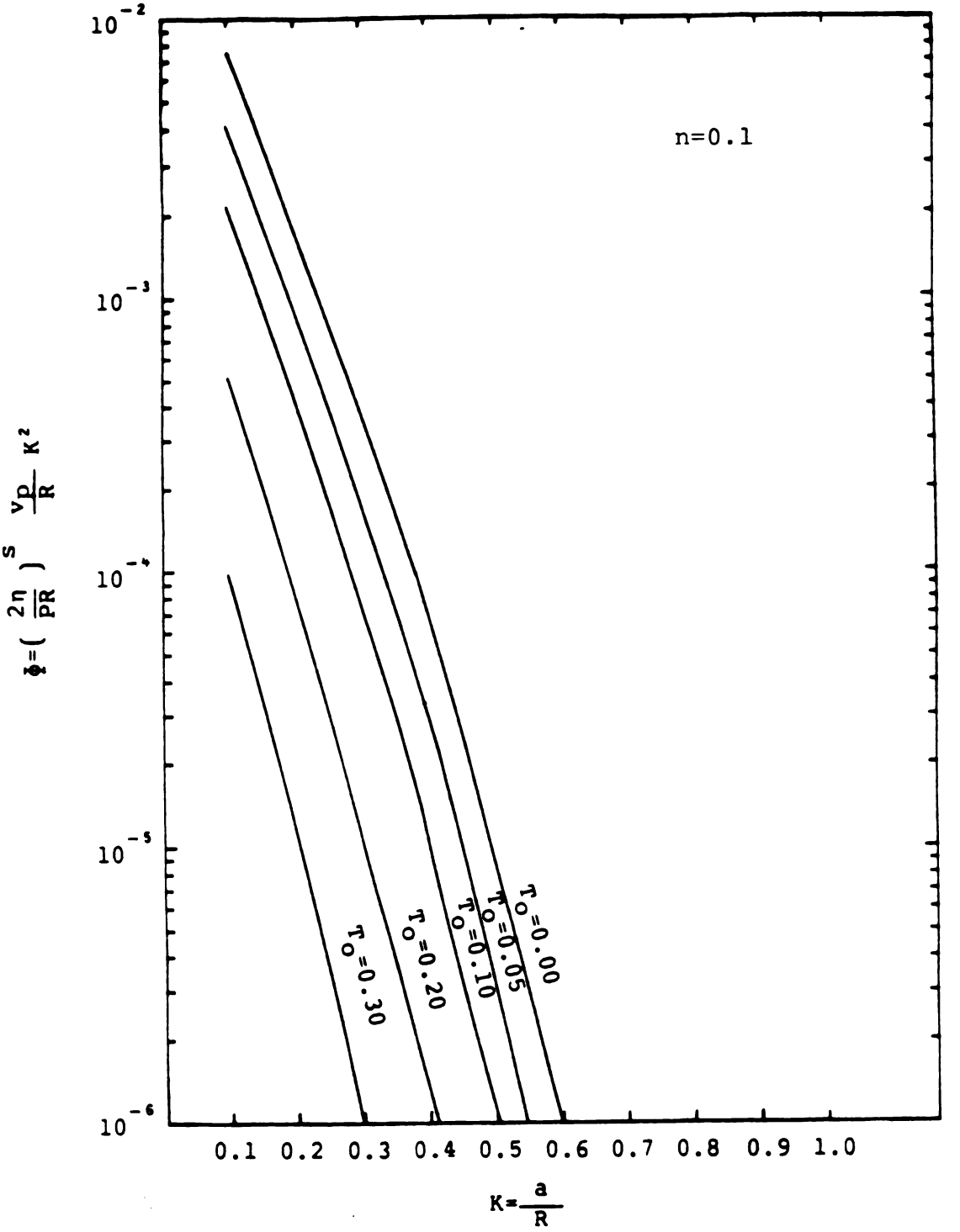

Figure 3. Dimensionless flow rate versus dimensionless plunger radius for n = 0.1.

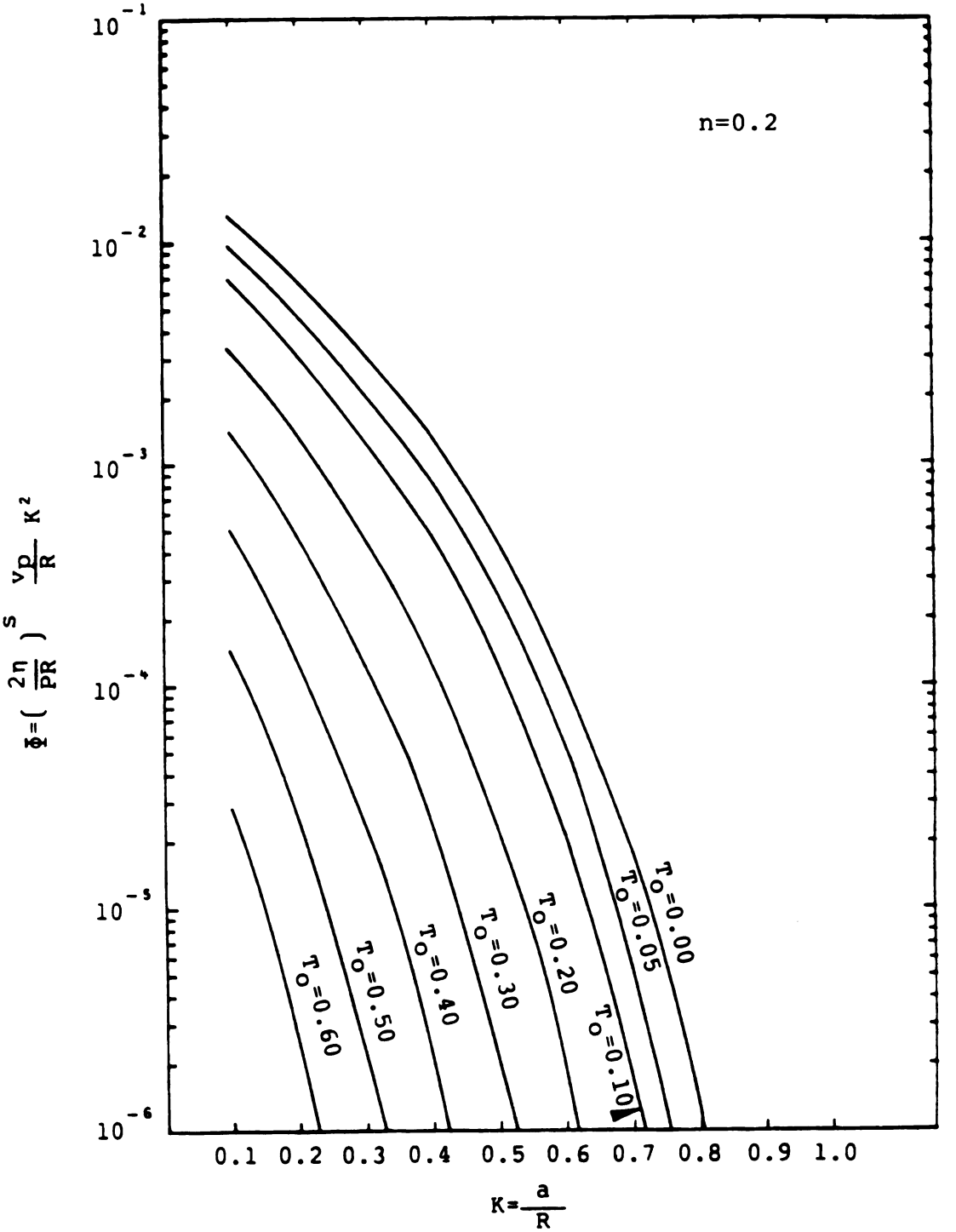

Figure 4. Dimensionless flow rate versus dimensionless plunger radius for n = 0.2.

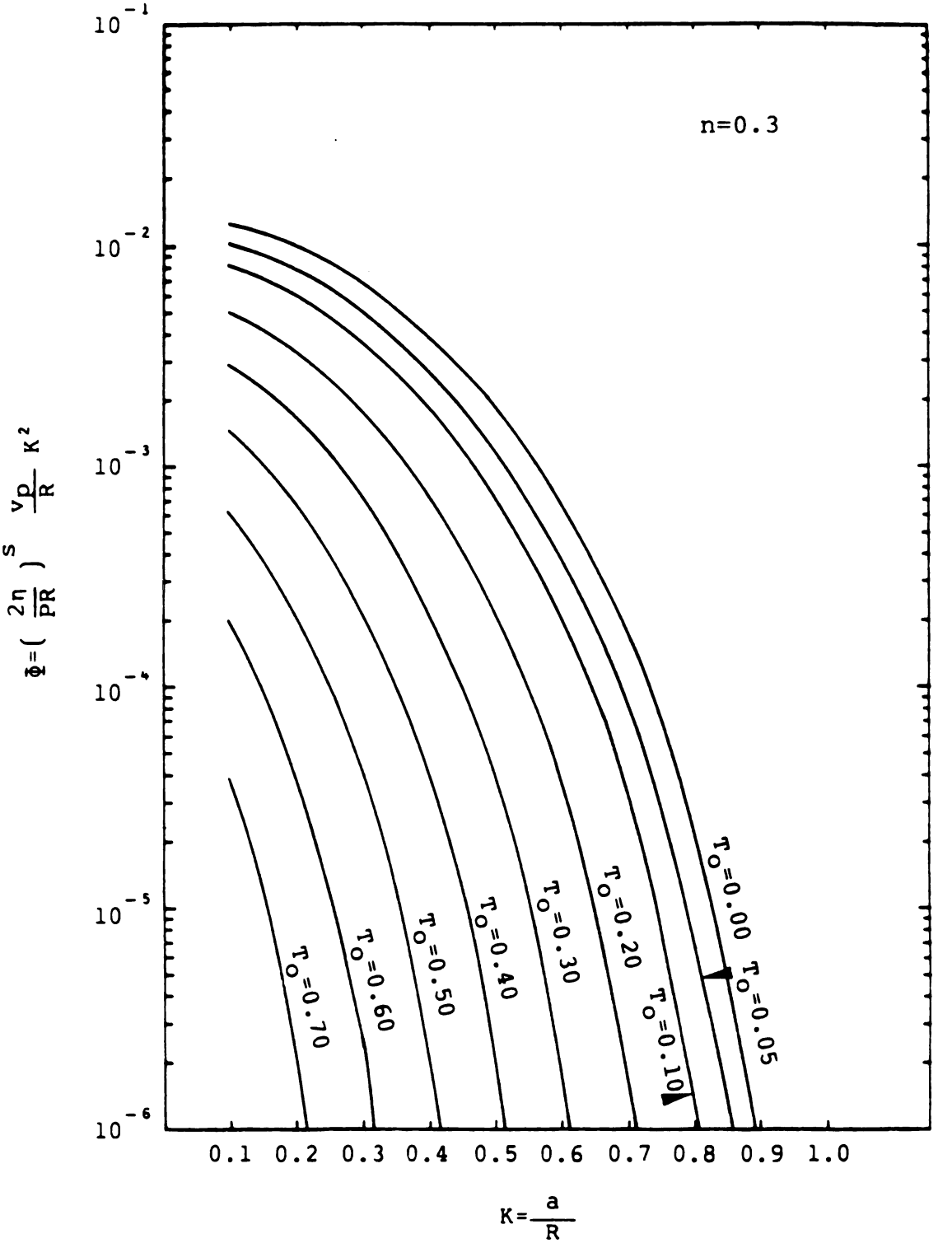

Figure 5. Dimensionless flow rate versus dimensionless plunger radius for n = 0.3.

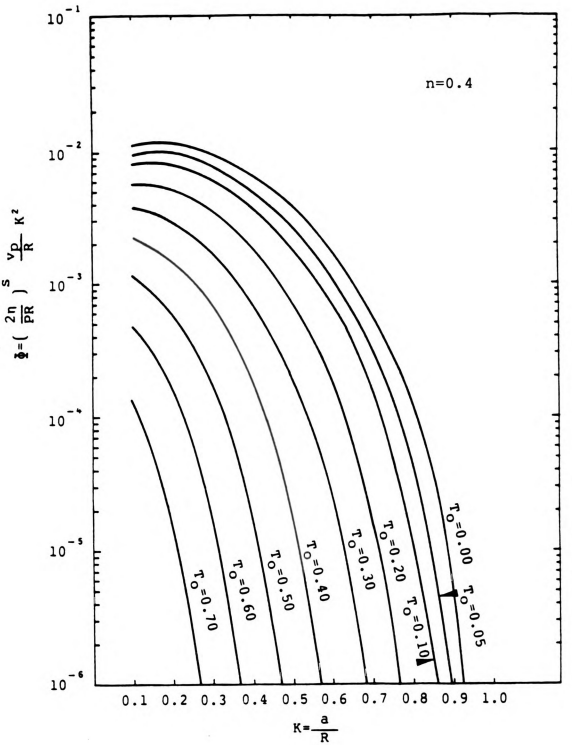

Figure 6. Dimensionless flow rate versus dimensionless plunger radius for n = 0.4.

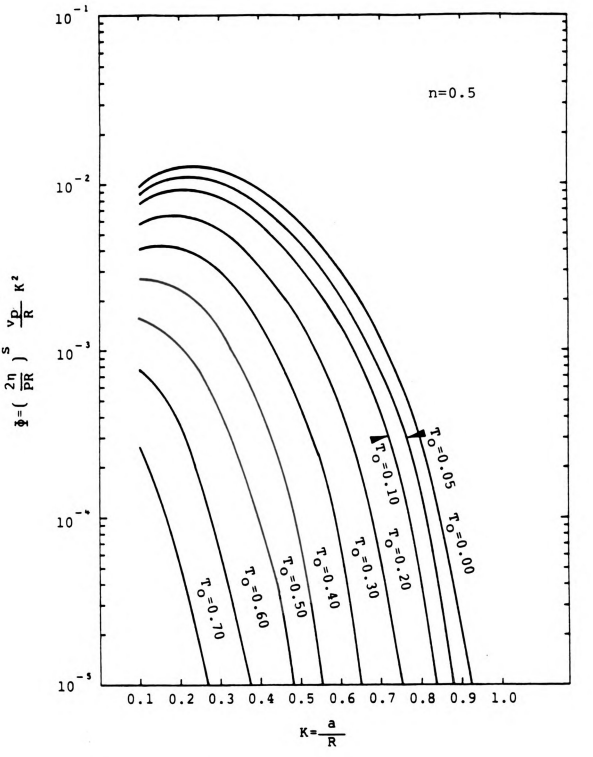

Figure 7. Dimensionless flow rate versus dimensionless plunger radius for n = 0.5.

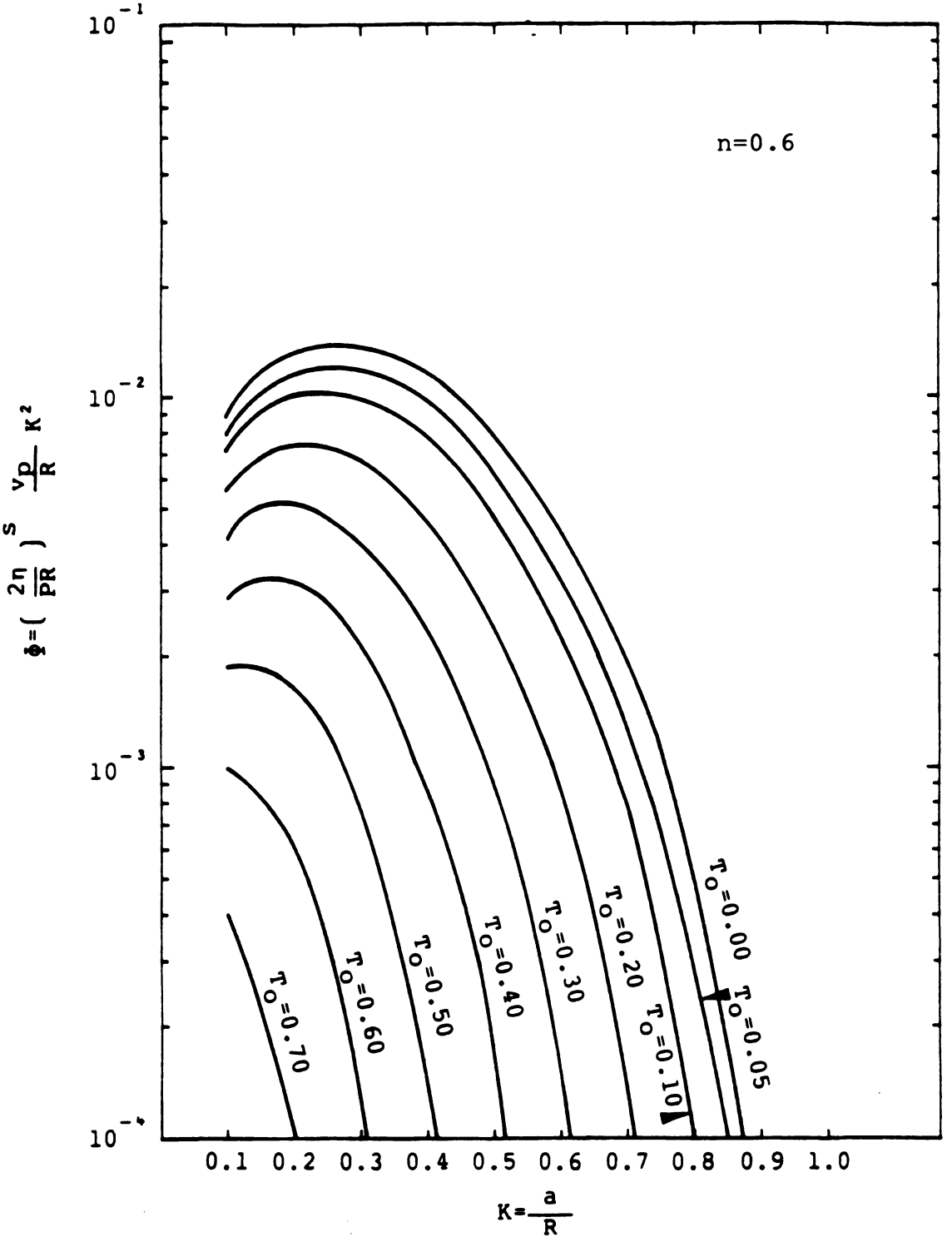

Figure 8. Dimensionless flow rate versus dimensionless plunger radius for n = 0.6.

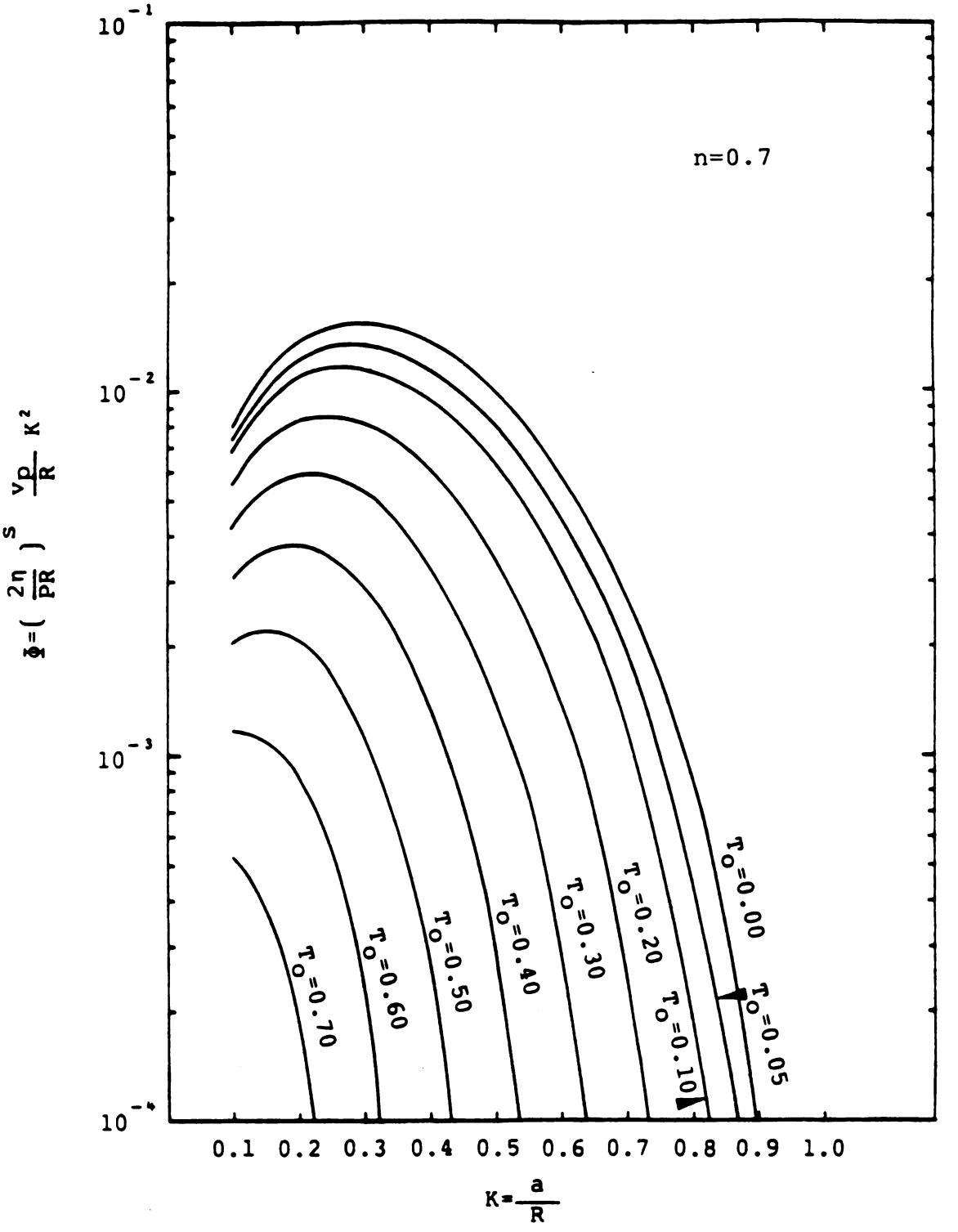

Figure 9. Dimensionless flow rate versus dimensionless plunger radius for n = 0.7.

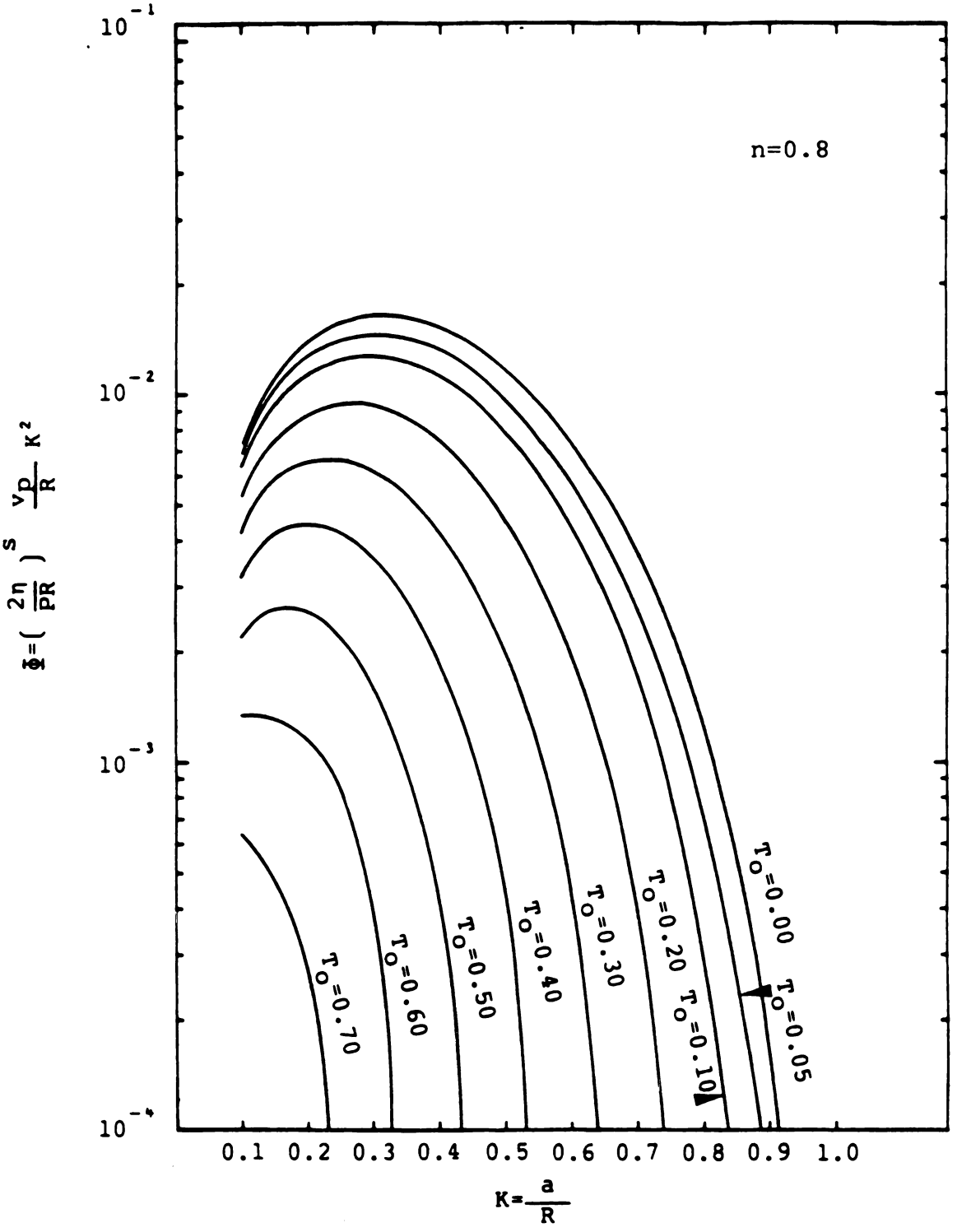

Figure 10. Dimensionless flow rate versus dimensionless plunger radius for n = 0.8.

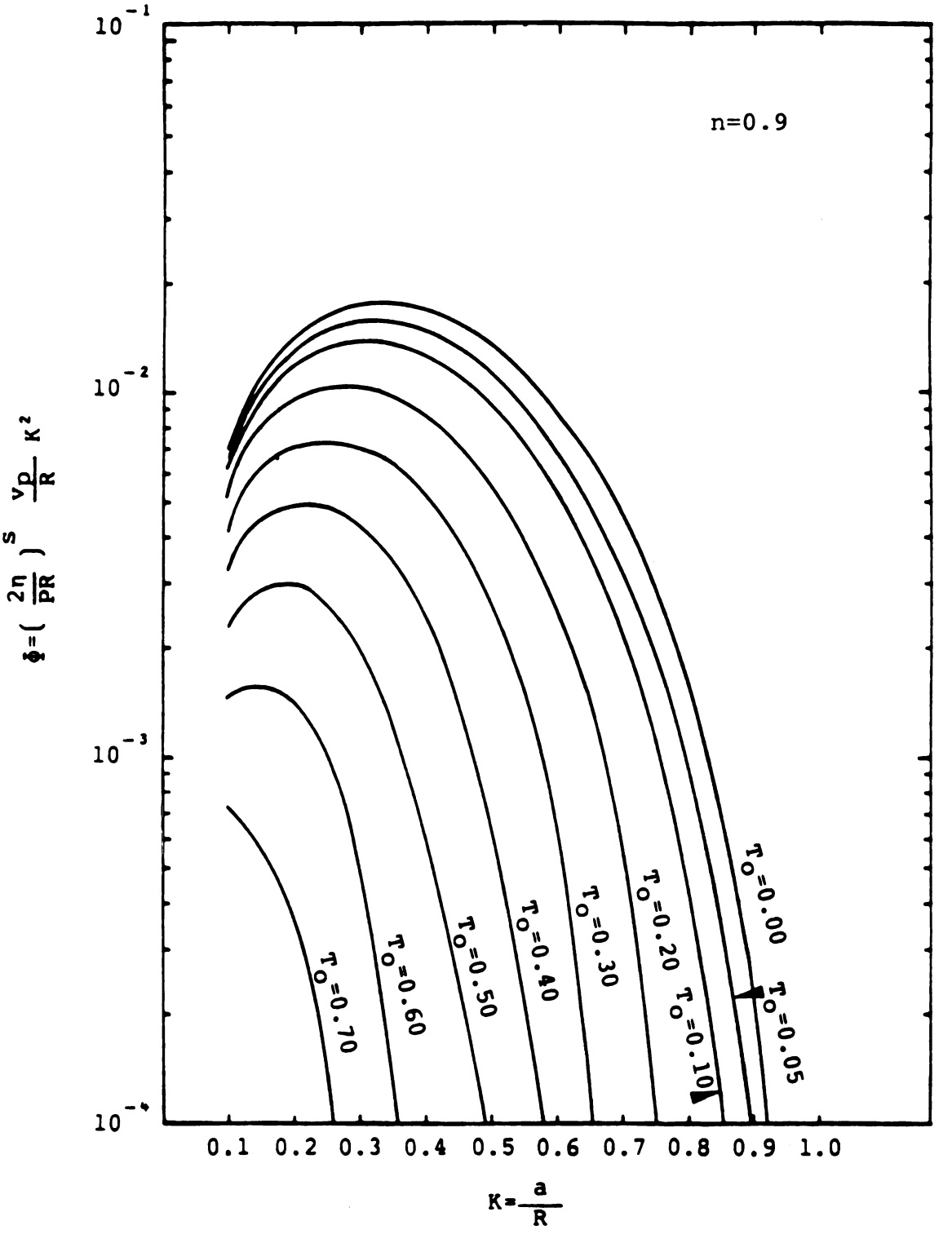

Figure 11. Dimensionless flow rate versus dimensionless plunger radius for n = 0.9.

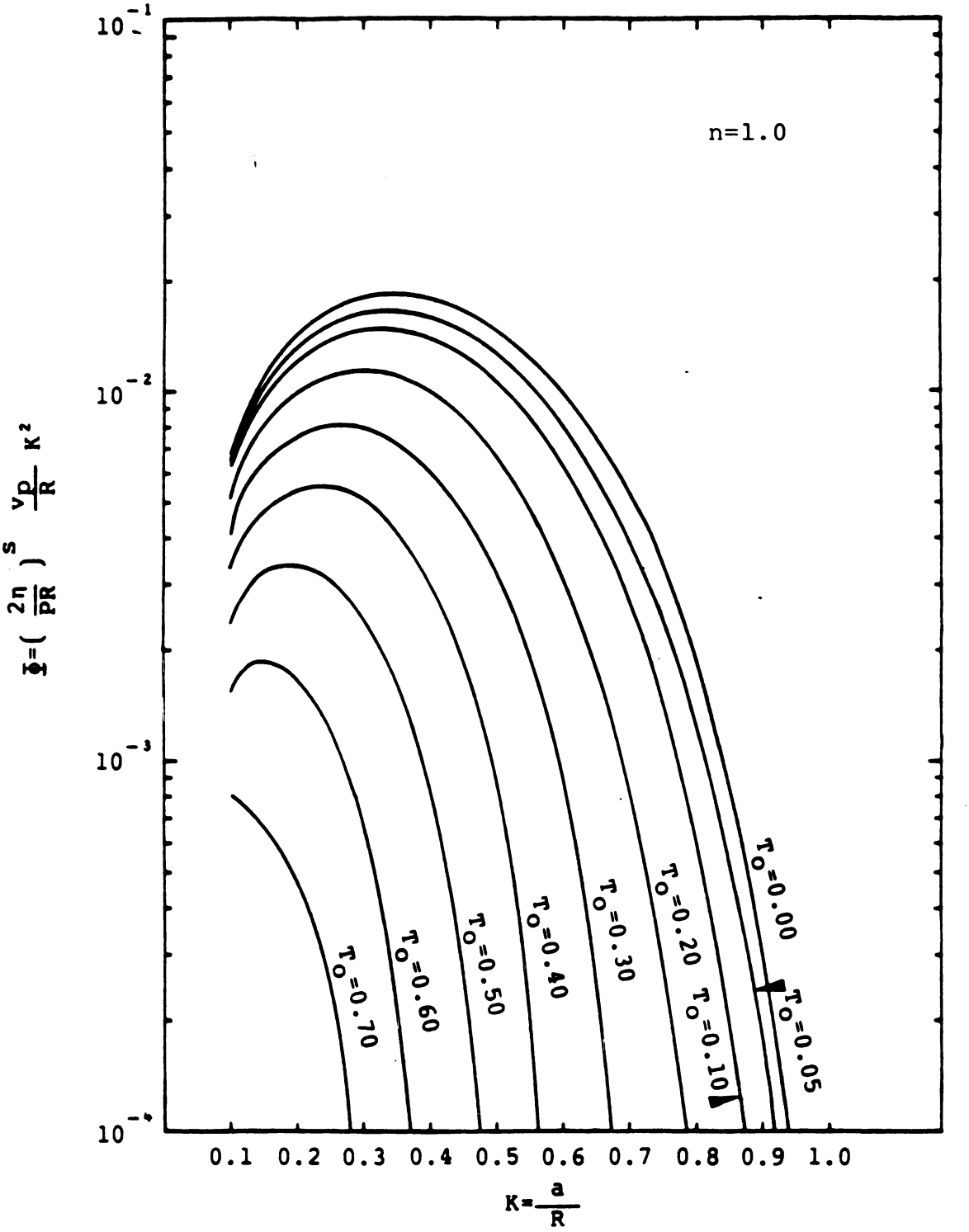

Figure 12. Dimensionless flow rate versus dimensionless plunger radius for n = 1.0.

$$\left(\frac{d\phi}{d\rho}\right)_{\rho=K} = \left(\frac{\lambda_+(\lambda_+ - T_o)}{K} - K - T_o\right)^s \qquad [45]$$

3.7 Special Solution for a Power Law Fluid

A simple solution was developed for the volumetric flow rate of a power law fluid in a back-extruder. For this special case, Equation [22] can be written as

$$T = \pm \left|\frac{d\phi}{d\rho}\right|^n \qquad [46]$$

and Equation [26] becomes

$$\lambda_- = \lambda_+ \qquad [47]$$

and Equation [28] becomes

$$\lambda^2 = \lambda_+^2 \qquad [48]$$

Velocity Profile

a) Region where $K < \rho < \lambda$

Equation [29] yields

$$\phi_- = \int_K^\rho \left(\frac{\lambda^2}{\rho} - \rho\right)^s d\rho - \phi_p \qquad [49]$$

where $s = 1/n$

b) Region where $\lambda < \rho < 1$

Equation [31] yields

$$\phi_+ = \int_{\rho}^{1} \left(\rho - \frac{\lambda^2}{\rho} \right)^s \, d\rho \qquad [50]$$

c) When $\rho = \lambda$

$$\int_K^{\lambda} \left(\frac{\lambda^2}{\rho} - \rho \right)^s \, d\rho - \int_{\lambda}^{1} \left(\rho - \frac{\lambda^2}{\rho} \right)^s \, d\rho = \phi_p \qquad [51]$$

The volumetric flow rate throug the annulus is given by

$$Q_T = 2\pi R^3 \left(\frac{2\eta}{PR} \right)^{-s} \int_K^1 \phi \rho d\rho = \pi R^3 \left(\frac{2\eta}{PR} \right)^{-s} \Phi \qquad [52]$$

where $\Phi = 2\int_K^1 \phi \rho d\rho$

Then, introducing Equations [49] and [50] into [52] gives

$$\Phi = 2\left\{ \int_K^{\lambda} \rho d\rho \int_K^{\rho} \left(\frac{\lambda^2}{\rho} - \rho \right)^s d\rho - \phi_p \int_K^{\lambda} \rho d\rho + \int_{\lambda}^{1} \rho d\rho \int_{\rho}^{1} \left(\rho - \frac{\lambda^2}{\rho} \right)^s d\rho \right\} \qquad [53]$$

By interchanging the order of integration in the above expression, the following is obtained:

$$\Phi = 2\left\{ \int_K^{\lambda} \left(\frac{\lambda^2}{\rho} - \rho \right)^s d\rho \int_{\rho}^{\lambda} \rho d\rho - \frac{\phi_p}{2} \left(\lambda^2 - K^2 \right) + \int_{\lambda}^{1} \left(\rho - \frac{\lambda^2}{\rho} \right)^s d\rho \int_{\lambda}^{\rho} \rho d\rho \right\}$$

Simplification yields

$$\Phi = 2\left[\int_K^{\lambda} \frac{1}{2} (\lambda^2 - \rho^2) \left(\frac{\lambda^2}{\rho} - \rho \right)^s d\rho - \frac{\phi_p}{2} (\lambda^2 - K^2) + \int_{\lambda}^{1} \frac{1}{2} (\rho^2 - \lambda^2) \left(\rho - \frac{\lambda^2}{\rho} \right)^s d\rho \right]$$

and more simplifications gives

$$\Phi = \int_K^1 |\lambda^2-\rho^2|^{s+1} \rho^{-s} d\rho - \phi_p [\lambda^2-K^2] \qquad [54]$$

The integral in Equation [54] may be evaluated analytically for arbitrary values of s. If the integrals in Equation [53] are integrated, each one by parts, the result is

$$\int_K^\lambda \rho d\rho \int_K^\rho \left(\frac{\lambda^2}{\rho} - \rho\right)^s d\rho = \frac{\lambda^2}{2} \int_K^\lambda \left(\frac{\lambda^2}{\rho} - \rho\right)^s d\rho - \frac{1}{2}\int_K^\lambda \rho^{2-s} (\lambda^2-\rho^2)^s d\rho \qquad [55]$$

and

$$\int_\lambda^1 \rho d\rho \int_\rho^1 \left(\rho - \frac{\lambda^2}{\rho}\right)^s d\rho = -\frac{\lambda^2}{2}\int_\lambda^1 \left(\rho - \frac{\lambda^2}{\rho}\right)^s d\rho + \frac{1}{2}\int_\lambda^1 \rho^{2-s} (\rho^2-\lambda^2)^s d\rho \qquad [56]$$

Placing Equations [55] and [56] into Equation [53] yields

$$\Phi = 2\left[\frac{\lambda^2}{2}\int_K^\lambda \left(\frac{\lambda^2}{\rho} - \rho\right)^s d\rho - \frac{\lambda^2}{2}\int_\lambda^1 \left(\rho - \frac{\lambda^2}{\rho}\right)^s d\rho - \right.$$
$$\left. - \frac{1}{2}\int_K^\lambda \rho^{2-s} (\lambda^2-\rho^2)^s d\rho + \frac{1}{2}\int_\lambda^1 \rho^{2-s} (\rho^2-\lambda^2)^s d\rho - \frac{\phi_p}{2}(\lambda^2-K^2)\right]$$

Introducing Equation [51] into the above expression results in

$$\Phi = \lambda^2\phi_p - \int_K^\lambda \rho^{2-s} (\lambda^2-\rho^2)^s d\rho + \int_\lambda^1 \rho^{2-s} (\rho^2-\lambda^2)^s d\rho - \phi_p (\lambda^2-K^2) \qquad [57]$$

Considering the integral $\int_K^\lambda \rho^{2-s} (\lambda^2-\rho^2)^s d\rho$ and choosing $u = \rho^{1-s}$ and $dv = (\lambda^2-\rho^2)^s \rho\, d\rho$ and integrating by parts yields

$$\int_K^\lambda \rho^{2-s} (\lambda^2-\rho^2)^s d\rho = \frac{1}{2}\left(\frac{1}{s+1}\right)\left[K^{1-s} (\lambda^2-K^2)^{(1+s)} + (1-s)\int_K^\lambda (\lambda^2-\rho^2)^{(s+1)} \rho^{-s} d\rho\right] \quad [58]$$

In a similar way, considering the integral $\int_\lambda^1 \rho^{2-s} (\rho^2-\lambda^2)^s d\rho$ and choosing $u = \rho^{1-s}$ and $dv = (\rho^2-\lambda^2)^s d\rho$ and integrating by parts yields

$$\int_\lambda^1 \rho^{2-s} (\rho^2-\lambda^2)^s d\rho = \frac{1}{2}\left(\frac{1}{s+1}\right)\left[(1-\lambda^2)^{(s+1)} - (1-s)\int_\lambda^1 (\rho^2-\lambda^2)^{(s+1)} \rho^{-s} d\rho\right] \quad [59]$$

Combining Equations [58] and [59] with Equation [57] and simplifying gives

$$\phi = K^2\phi_p - \frac{1}{2}\left(\frac{1}{s+1}\right)\left[K^{1-s} (\lambda^2-K^2)^{(1+s)} + (1-s)\int_K^\lambda (\lambda^2-\rho^2)^{(s+1)} \rho^{-s} d\rho\right] + \frac{1}{2}\left(\frac{1}{s+1}\right)\left[(1-\lambda^2)^{(s+1)} - (1-s)\int_\lambda^1 (\rho^2-\lambda^2)^{(s+1)} \rho^{-s} d\rho\right]$$

$$\phi = K^2\phi_p - \frac{1}{2}\left(\frac{1}{s+1}\right)\left[K^{1-s} (\lambda^2-K^2)^{(1+s)} - (1-\lambda^2)^{(s+1)} - (1-s)\int_K^1 |\lambda^2-\rho^2|^{(s+1)} \rho^{-s} d\rho\right] \quad [60]$$

Equation [60] must be equal to Equation [54], or

$$2(s+1)\int_K^1 |\lambda^2-\rho^2|^{s+1}\rho^{-s}d\rho - (2\phi_p(\lambda^2-K^2) + 2K^2\phi_p(s+1) =$$

$$= -(K^{1-s}(\lambda^2-K^2)^{(1+s)} - (1-\lambda^2)^{(s+1)} - (1-s)\int_K^1 |\lambda^2-\rho^2|^{(s+1)}\rho^{-s}d\rho$$

Simplifying this expression gives

$$\int_K^1 |\lambda^2-\rho^2|^{s+1}\rho^{-s}d\rho = \frac{1}{s+3}\left[(1-\lambda^2)^{s+1} - K^{(1-s)}(\lambda^2-K^2)^{1+s} + 2(s+1)\phi_p(\lambda^2)\right] \quad [61]$$

Placing Equation [61] into Equation [54] yields

$$\phi = \frac{1}{s+3}\left[(1-\lambda^2)^{(s+1)} - K^{(1-s)}(\lambda^2-K^2)^{1+s}\right] + \frac{2(s+1)}{(s+3)}\phi_p(\lambda^2) - \phi_p(\lambda^2-K^2)$$

Then, with final algebraic simplfication, the analytical equation for volumetric flow rate of a power law fluid in a back-extruder is

$$Q_T = \pi R^3\left(\frac{PR}{2\eta}\right)^s\left[\frac{1}{s+3}\left((1-\lambda^2)^{(s+1)} - K^{(1-s)}(\lambda^2-K^2)^{1+s}\right) + \right.$$

$$\left. + \phi_p\left(\frac{2(s+1)}{(s+3)}\lambda^2 - (\lambda^2-K^2)\right)\right] \quad [62]$$

For the case of a power law fluid, the values of the limit of the plug region (λ_+) are obtained from Table 1 using the fact that the dimensionless yield stress (T_o) is zero; then using Equation [27], the value of the constant of integration (λ) is known.

The dimensionless flow rate (Φ) for a power law fluid is obtained from Figures (3) to (12) with the dimensionless yield stress (T_o) equal to zero. The dimensionless velocity at the plunger wall (ϕ_p) is then calculated with Equation [43].

Chapter 4

Experimental Applications

4.1 Materials and Methods

To test the mathematical model for non-Newtonian flow in a back-extrusion device, laboratory experiments were conducted using graduate cylinders of different diameters as sample holders, and plexiglass plunger rods with different diameters. A model TT-BM Instron Universal Testing machine was used to operate the plunger. The plunger was screwed to the cross-head of the Instron and the compression load cell was located in the Instron loading platform. The graduate cylinder containing the sample was placed on the top of the compression load cell. A strip-chart was used to record force as a function of time (position).

The test fluids employed during the experiments were aqueous solutions of Methocel K15MS (hydroxypropyl-methyl-cellulose) from the Dow Chemical Co.--because it behaves as a power law fluid--and aqueous solutions of Kelset (sodium-calcium alginate) from Kelco Co. as a model for a Herschel-Bulkley fluid. Fundamental fluid properties were characterized in the form of shear stress versus shear rate on a Haake RV-12 viscometer, interfaced to a Hewlett-Packard 85 computer and 3497 data acquisition system. The MV-I, MV-II, MV-III and SV-I concentric cylinder sensors were utilized in conjunction with the MV paddle mixer (or impeller) to determine rheological properties of the aqueous solution of Methocel K15MS; the samples were held in the MV

cup for all tests. Due to the high torque values presented by the aqueous solution of Kelset, rheological properties were determined by using only the MV paddle mixer and MV cup. The procedure used to determine the rheological properties was the same as that described by Ford and Steffe (1984).

4.2 Data Analysis Procedure

4.2.1 Analytical Determination of Buoyancy Force

Buoyancy force can be calculated analytically. Consider Figure 13 showing the plunger at zero velocity.

At equilibrium, the force on the plunger is

$$F_b = \Delta P_b \pi a^2 \qquad [63]$$

and the hydrostatic pressure

$$\Delta P_b = \gamma_1 \, g \, L \qquad [64]$$

The length of rod that penetrated the fluid is $\overline{OB}$, and the volume displaced by the rod is equal to $\pi a^2 \overline{OB}$. The displaced volume is forced up around the annulus, so the following relationship is valid

$$\pi a^2 \, \overline{OB} = \pi R^2 \, \overline{AO} - \pi a^2 \, \overline{AO}$$

or

$$\overline{AO} = \frac{a^2}{(R^2 - a^2)} \, \overline{OB} \qquad [65]$$

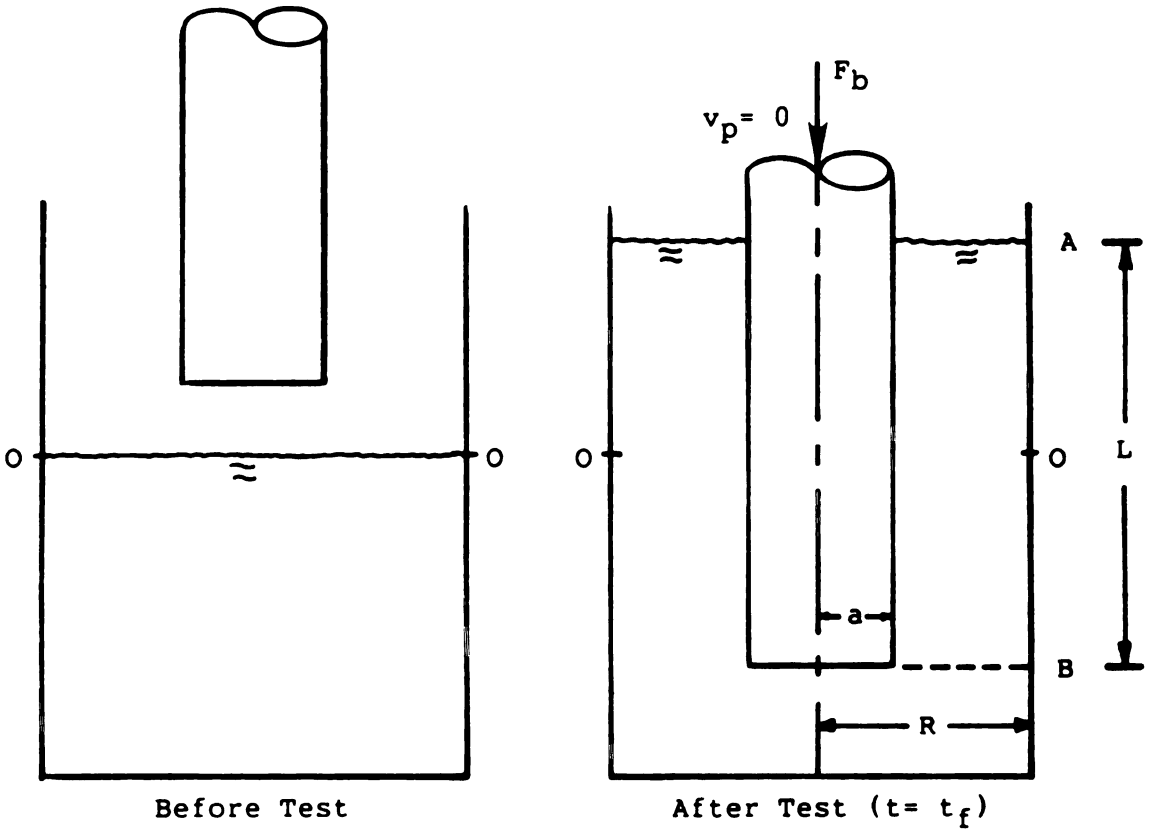

Figure 13. Position of the plunger before and after completion of testing.

also,

$$L = \overline{AO} + \overline{OB} \qquad [66]$$

Placing Equation [65] into Equation [66] and rearranging yield a value for L as

$$L = \frac{\overline{OB}}{1-K^2} \qquad [67]$$

Substituting this relation into Equation [63] results in

$$F_b = \gamma_1 \, g \, \frac{\overline{OB}}{(1-K^2)} \, \pi a^2 \qquad [68]$$

$\overline{OB}$ can be measured or it can be calculated as

$$\overline{OB} = \frac{l_{ch}}{C_{sp}} \, v_p \qquad [69]$$

where

l_{ch} = chart length, obtained from the recorder, m

C_{sp} = chart speed of the recorder, m/s

v_p = velocity of the plunger, m/s

With $\overline{OB}$ obtained from Equation [69], it is possible to calculate L by using Equation [67].

4.2.2 Force Balance on Plunger

When the plunger is forced down into the sample, fluid flows upward in the annulus. At a constant plunger velocity, the total force applied in the plunger is equal to

the force due to the shear stress on the plunger wall plus the force due to static pressure pushing upward on the bottom surface of the plunger. Static force at the base of the plunger, composed of buoyancy force and the force responsible for fluid flow in the upward direction (Morgan et al., 1979), may be expressed as

$$F_T = 2\pi a\ L\ \tau_w + \pi a^2 \Delta P + \gamma g L \pi a^2 \qquad [70]$$

where $\gamma g L \pi a^2$ = hydrostatic or buoyancy force = F_b, N

F_T = force applied on the plunger, N

$2\pi a L \tau_w$ = force due to the shear stress at the wall, N

$\pi a^2 \Delta P$ = force responsible for fluid flow in the upward direction

The force corrected for buoyancy (F_{cb}) may be defined as

$$F_{cb} = F_T - \gamma g L \pi a^2 \qquad [71]$$

Then, with simplification,

$$F_{cb} = 2\pi a L\ \tau_w + \pi a^2 \Delta P \qquad [72]$$

Rearranging Equation [72] as

$$\frac{F_{cb}}{L} = 2\pi\ a\ \tau_w + \pi a^2 \left(\frac{\Delta P}{L}\right)$$

and dividing both sides by $\pi\ (\frac{\Delta P}{L})$ Ra, and using Equations [14] and [11] and the definition of K as $K = \frac{a}{R}$ yields

$$\frac{F_{cb}}{\pi LPRa} = T_w + K \qquad [73]$$

This equation is very important because it relates the force corrected for buoyancy (F_{cb}) being applied to the plunger to the dimensionless shear stres at the wall (T_w), the pressure drop per unit of length (P), and the geometric dimensions of the rod and cylinder containing the fluid.

Equation [73] is fundamental when back extrusion technique is used to determine rheological properties of a given fluid.

4.2.3 Determination of Yield Stress

From Equation [70], the total force applied to the plunger is

$$F_T = 2\pi aL\ \tau_w + \pi a^2 \Delta P + F_b$$

and using Equation [7], this may be expressed as

$$F_T = 2\pi aL\ \tau_y + 2\pi aL\eta\ \left(\frac{dv}{dr}\right)^n_{r=a} + \pi a^2 \Delta P + F_b \qquad [74]$$

When the plunger is stopped in the fluid, the situation depicted in Figure 14 is obtained and Equation [74] becomes, when $v_p = 0$,

$$F_{T_e} = 2\pi aL\ \tau_y + F_b \qquad [75]$$

F_b can be analytically determined by using Equation [68];

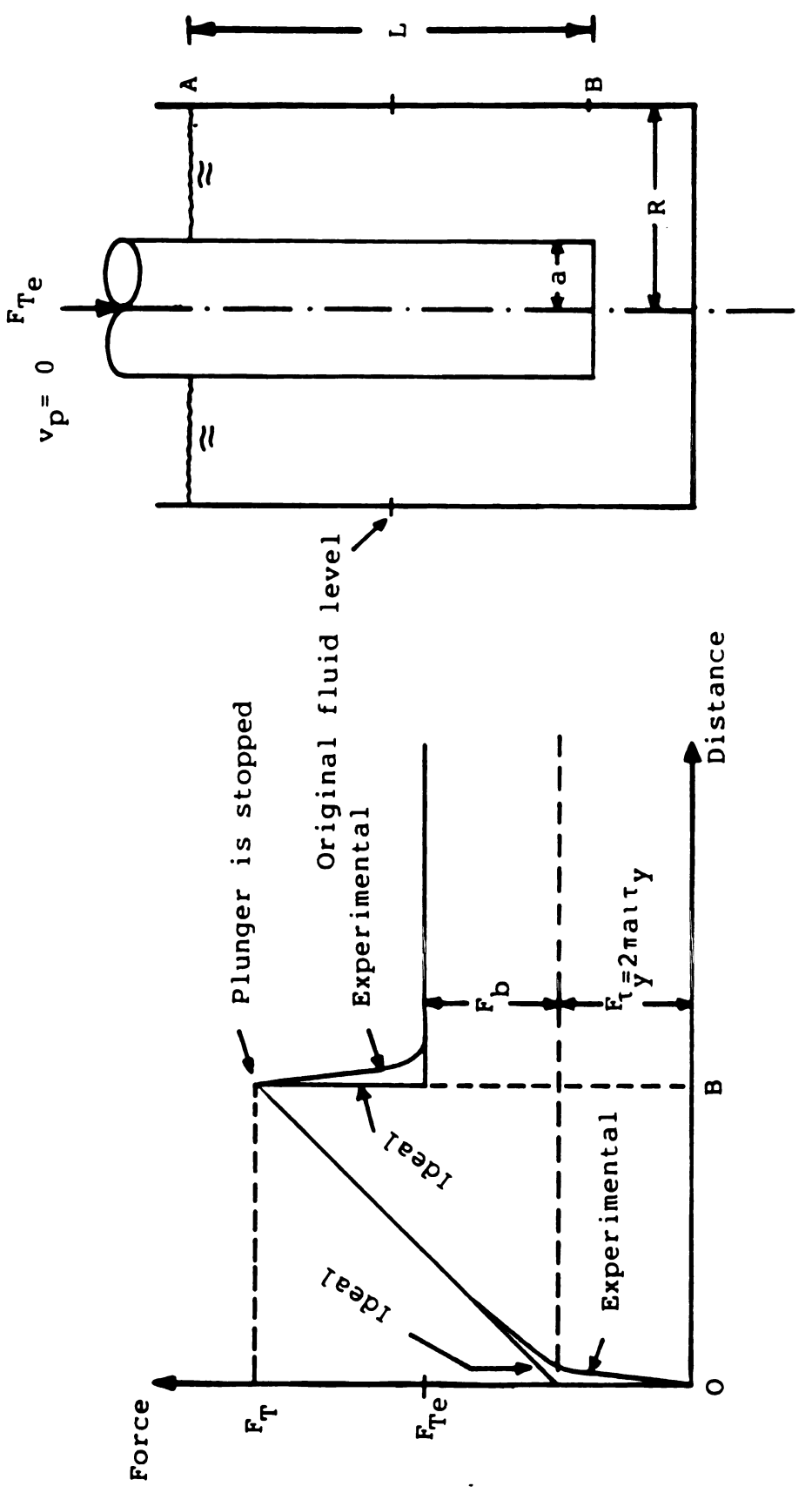

Figure 14. Force versus distance diagram of a Herschel-Bulkley fluid.

and F_{T_e} is the recorded force after the plunger is stopped.

Then, the yield stress (τ_y) can be calculated as

$$\tau_y = \frac{F_{T_e} - F_b}{2\pi aL} \qquad [76]$$

4.2.4 Determination of Rheological Properties of a Power-Law Fluid

4.2.4.1 Determination of the Flow Behavior Index

Combining Equations [37] and [42] yields

$$\phi = \left(\frac{2\eta}{PR}\right)^s \frac{v_p}{R} K^2 \qquad [77]$$

If a power law fluid is tested in a back-extrusion device at two different plunger velocities (v_p), then Equation [77] may be written as

$$\phi_1 = \left(\frac{2\eta}{P_1 R_1}\right)^s \frac{v_{p1}}{R_1} K_1^2$$

for the first test, and

$$\phi_2 = \left(\frac{2\eta}{P_2 R_2}\right)^s \frac{v_{p2}}{R_2} K_2^2$$

for the second test.

If the plunger and cylinder are the same in both experiments then the dimensionless radius (K) is constant in both tests as is R. In this case, the ratio ϕ_1/ϕ_2 will be equal to one--as it can be seen from Figures 3 to 12, for a power law fluid--which means the dimensionless yield stress (T_o) is zero, i.e.

$$\frac{\Phi_1}{\Phi_2} = \left(\frac{P_2}{P_1} \right)^s \frac{v_{p1}}{v_{p2}} = 1 \qquad [78]$$

Note, Equation [78] is valid only for Newtonian and power law fluids.

On the other hand, from Equation [73],

$$\frac{F_{cb1}}{\pi L_1 P_1 R_1 a_1} = T_{w1} + K_1$$

for the first run, and

$$\frac{F_{cb2}}{\pi L_2 P_2 R_2 a_2} = T_{w2} + K_2$$

for the second run.

If the plunger and cylinder are the same in both experiments then, the dimensionless radius (K) is constant as are the plunger radius (a) and cylinder radius (R). From Equation [44], it is easily shown that (for a power law fluid) the dimensionless shear stress (T_w) is constant because T_o equals zero and K, R and a are constants in both tests. Then, the ratio of the forces corrected for buoyancy may be written as

$$\frac{F_{cb1}}{F_{cb2}} \frac{L_2}{L_1} \frac{P_2}{P_1} = 1 \qquad [79]$$

Like Equation [78], equation [79] is valid only for Newtonian and power law fluids.

Solving for P_2/P_1 in Equation [79], then placing this value into Equation [78], rearranging and taking logarithms yields

$$s = \frac{\ln\left(\frac{v_{p2}}{v_{p1}}\right)}{\ln\left(\frac{F_{cb2}}{F_{cb1}} \cdot \frac{L_1}{L_2}\right)} \qquad [80]$$

Using Equation [80] it is possible to determine the flow behavior index which was previously defined as n = 1/s.

4.2.4.2 Determination of the Shear Stress at the Plunger Wall

Knowing the flow behavior index (n), the geometry of the system ($K = \frac{a}{R}$), and the fact that for a power-law fluid $T_o = \frac{2\tau_y}{PR} = 0$, it is possible to determine λ_+ from Table 1. With the appropriate value of λ_+ and by using Equation [44], the dimensionless shear stress at the wall is easily computed. Replacing the known values in Equation [73], with the force corrected for buoyancy (Fcb) obtained experimentally, the pressure drop per unit of length, P, is first calculated. Finally, with Equation [11] the shear stress at the plunger wall, τ_w, is obtained as $\tau_w = \frac{PRT_w}{2}$

4.2.4.3 Determination of the Consistency Coefficient

The consistency coefficient, η, is determined knowing the flow behavior index and K, and using the appropriate graphic (Φ vs. K) with $T_o = 0$ and n as a parameter. Recall that these graphic solutions are presented in Figures 3 to 12.

With P calculated before--during the determination of the shear stress at the plunger wall--and by using the known values in Equation [77], the consistency coefficient n is obtained as

$$\eta = \frac{PR}{2}\left(\frac{\Phi R}{v_p K_2}\right)^n$$

4.2.4.4 Determination of the Shear Rate at the Plunger Wall

Equation [13] gives the definition of the dimensionless velocity as

$$\phi = \left(\frac{2\eta}{PR^{n+1}}\right)^{1/n} v$$

Differentiating this equation with respect to ρ, where $\rho = \frac{r}{R}$ yields

$$\frac{d\phi}{d\rho} = \left(\frac{2\eta}{PR^{n+1}}\right)^{1/n} \frac{dv}{d\rho}$$

and simplification gives

$$\frac{d\phi}{d\rho} = \left(\frac{2\eta}{PR}\right)^{1/n} \frac{1}{R} \frac{dv}{d\rho}$$

Since $Rd\rho = dr$, the final expression for the derivative may be written as

$$\frac{d\phi}{d\rho} = \left(\frac{2\eta}{PR}\right)^{1/n} \frac{dv}{dr} \qquad [81]$$

Evaluating Equation [81] at r = a yields the shear rate at the plunger wall as

$$\left.\frac{dv}{dr}\right|_{r=a} = \left(\frac{PR}{2\eta}\right)^{1/n} \left(\frac{d\phi}{d\rho}\right)_{\rho=K} \qquad [82]$$

For a power law fluid, the dimensionless shear rate at the wall ($(\frac{d\phi}{d\rho})_{\rho = K}$) is obtained with the λ_+ value calculated before--during the determination of the shear

stress at the plunger wall--and Equation [45] with $T_o = 0$. Then, Equation [82] is used to obtain the shear rate at the plunger wall using the other known values.

4.2.5 Determination of Rheological Properties of a Bingham Plastic Fluid

4.2.5.1 Determination of the Yield Stress and Plastic Viscosity

For a Bingham plastic fluid, the flow behavior index, n, is equal to one. The yield stress for this fluid is obtained by using Equation [76] and the following steps are required to determine the plastic viscosity, η_p:

1. For a given plunger velocity vp, calculate the quantity

$$\frac{F_{cb}}{\pi LRa}$$

From Equation [73], this quantity may be expressed in terms of P, T_w and K as

$$\frac{F_{cb}}{\pi LRa} = P\ (T_w + K) \qquad [73a]$$

2. Assume a value for the dimensionless yield stress To;
3. Using Equation [12] determine the pressure drop per unit of length P;
4. With To and K use Figure 12 (with n = 1.0) to determine Φ;
5. Use Table 1 to determine λ^+;
6. Use Equation [44] to determine T_w;
7. Use Equation [77] to determine η_p;
8. Compute the expression $P\ (T_w + K)$ and verify if Equation

[73a] is satisfieid. If the equation is not, return to step 2. If Equation [73a] is satisfied, the correct value of the plastic viscosity was calculated in step 7. For a new plunger velocity vp, return to step 1.

4.2.5.2 Determination of the Shear Rate at the Plunger Wall

To determine the shear rate at the plunger wall for a Bingham plastic fluid, Equation [82] is used with the known values calculated before for P, and η_p, with n = 1. The dimensionless shear rate is calculated with the λ_+ value calculated in step 5 and Equation [45], using the To value that satisfied Equation [73a].

4.2.5.3 Determination of the Shear Stress at the Plunger Wall

The shear stress at the plunger wall (τ_w) is obtained from the dimensionless shear stress at the wall (T_w) and using Equation [11] with the known values of P, R and τ_w expressed as

$$\tau_w = \frac{PRT_w}{2}$$

4.2.6 Determination of Rheological Properties of a Herschel-Bulkley Fluid

The rheological properties of a Herschel-Bulkley fluid may be determined from the following steps:

1. For a given plunger velocity v_p, determine the expression $\frac{F_{cb}}{\pi LRa}$, where F_{cb} is obtained from Equation [71]. The above quantity may be expressed in terms of P, T_w and K as

$$\frac{F_{cb}}{\pi LRa} = P\ (T_w + K) \qquad [73a]$$

2. Assume a value for the flow behavior index n;
3. Assume a value for the dimensionless yield stress T_o;
4. Using Equation [12] determine the pressure drop per unit of length P, with the value of yield stress (τ_y) obtained from Equation [76];
5. With T_o and K use the appropriate graphic from Figures 3 to 12 to determine Φ;
6. Use Table 1 to determine λ_+;
7. Use Equation [44] to determine T_w;
8. Use Equation [77] to determine η;
9. Compute the expression $P\ (T_w + K)$;
10. Return to step 3, in order to obtain at least three values of $P\ (T_w + K)$ and η at a given n;
11. Return to step 2, to plot the necessary curves at different n values that cover the range needed to obtain the correct n value;
12. Plot the values of $P\ (T_w + K)$ versus η with n as parameter;
13. Draw the line corresponding to the value of $\frac{F_{cb}}{\pi LRa}$ computed in step 1;
14. Use a new plunger velocity vp and repeat steps 1 to 13 for this new value of v_p.

The rheological properties of the fluid are found when, for a specific flow behavior index n, the consistency coefficient is the same in both curves at two different plunger velocities as illustrated in Figure 15.

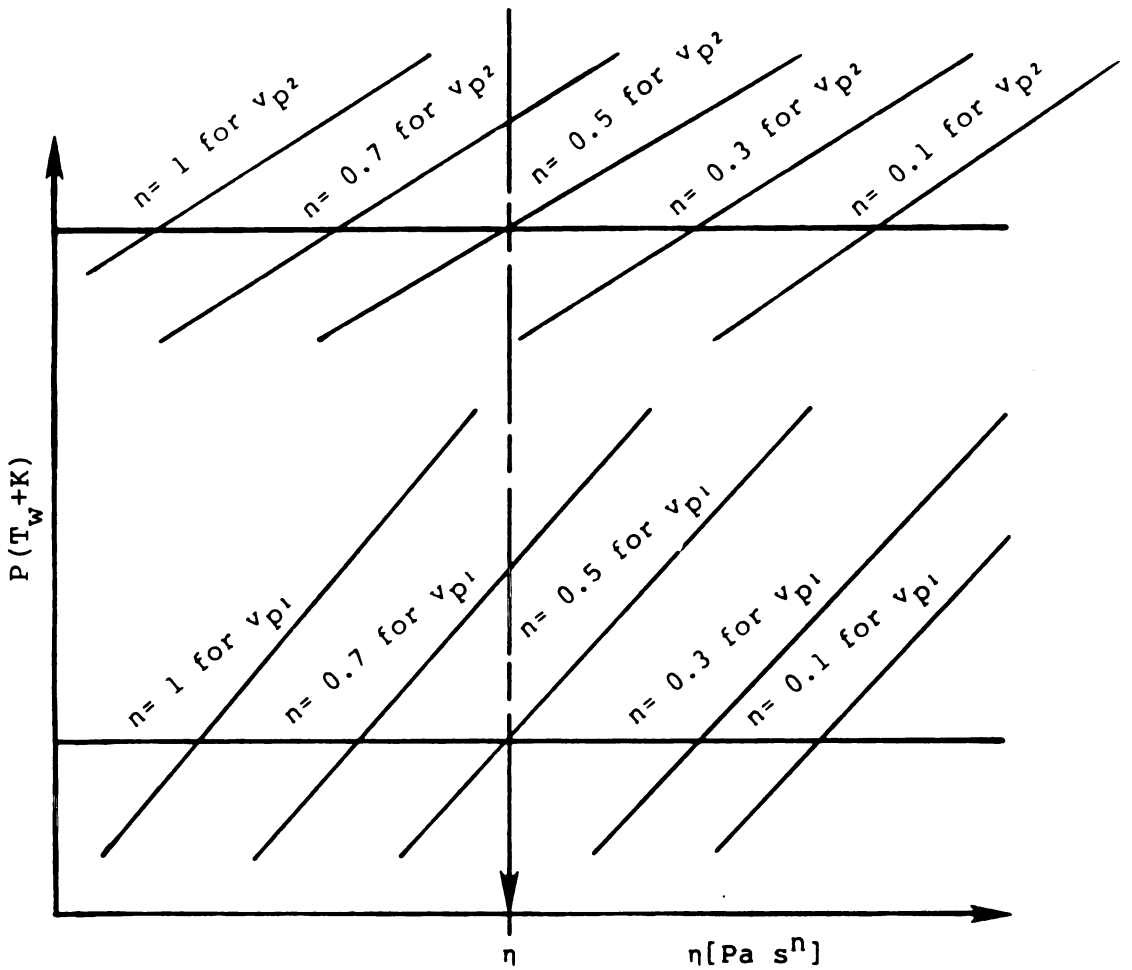

Figure 15. Illustration of the method for determining rheological properties of a Herschel-Bulkley fluid with the back-extrusion technique.

With n and η known, the shear stress at the wall may be computed using the values of T_o and λ_+ obtained at either vp1 or vp2 for the known flow behavior index n. Equations [45] and [82] are used to calculate the dimensionless shear rate and the actual shear rate, at the plunger wall, respectively. Also, equations [44] and [11] are used to determine the dimensionless shear stress and the actual shear stress, and the plunger wall, respectively.

4.2.7 Determination of Rheological Properties of a Newtonian Fluid

For a Newtonian fluid, the dimensionless yield stress (T_o) value is zero, and the flow behavior index (n) is one.

4.2.7.1 Determinaton of Viscosity

With a given dimensionles radius (K), the value of λ_+ is obtained from Table 1. Placing the value of λ_+ into Equation [44]--using T_o = 0--the dimensionless shear stress at the wall (T_w) is obtained. After calculating the force corrected for buoyancy force (F_{cb}) with Equation [71], calculate the pressure drop per unit of length using Equation [73], for a given plunger velocity (v_p).

Use Figure [12] to obtain the dimensionless volumetric flow rate (Φ). Placing the known values into Equation [77], the viscosity is obtained as

$$\eta = \mu = \frac{PR^2}{2} \frac{\Phi}{v_p K^2}$$

4.2.7.2 Determination of the Shear Rate at the Plunger Wall

Use Equation [45] to determine the dimensionless shear rate at the plunger wall ($(\frac{d\phi}{d\rho})_{\rho=K}$). Recall that s = 1/n = 1 for a Newtonian fluid and $T_o = 0$. Use the λ_+ value as obtained in 4.2.7.1.

Placing the known values into Equation [82], the shear rate at the plunger wall is obtained.

4.2.7.3 Determination of the Shear Stress at the Plunger Wall

Placing the known values into Equation [11], the shear stress at the plunger wall (τ_w) is computed as

$$\tau_w = \frac{PRT_w}{2}$$

Chapter 5

RESULTS AND DISCUSSION

To validate the mathematical model, experiments were conducted with two types of fluids. Methocel aqueous solutions--used as power law fluids--and Kelset aqueous solutions--used as Herschel-Bulkley fluids.

5.1 Power Law Fluids

When using Methocel solutions as power law fluids, the force versus distance diagrams obtained with the chart recorder were straight lines through the origin of the the coordinates. When the plunger was stopped, the force recorded dropped sharply to a constant value of force--the buoyancy force--indicating that the fluid did not exhibit time-dependent behavior. The buoyancy force value obtained from the chart recorder was the same as that predicted using Equation (68), as seen in Table 2.

Table 2 also shows that the predicted values of L, F_b, and OB are the same as those measured experimentally. From the above, Equations (67), (68) and (69) can be used to predict the length of the annular region (L), the buoyancy force (F_b) and the position of the lower surface of the plunger ($\overline{OB}$) respectively.

The values of s--the inverse of the flow behavior index (n)--calculated by using Equation (80) are presented in Table 3 for experiments A, B, C and D. The values of λ_+, T_w, $\left(\frac{d\phi}{d\rho}\right)_{p=K}$ and ϕ--calculated using the average value of n from experiments A, B, C, D--were computed following the

Table 2. Experimental and predicted values obtained for a power law fluid.

	EXPERIMENT			
	A	B	C	D
v_p, m/s	$1.6667 \cdot 10^{-5}$	$8.333 \cdot 10^{-4}$	$16.667 \cdot 10^{-4}$	$83.333 \cdot 10^{-4}$
C_{sp}, m/s	$5.00 \cdot 10^{-4}$	$33.333 \cdot 10^{-4}$	$33.333 \cdot 10^{-4}$	$83.333 \cdot 10^{-4}$
l_{ch}, m	0.24	0.332	0.157	0.082
$\overline{OB}_{measured}$, m	0.0815	0.080	0.080	0.082
$\overline{OB}_{calc.}$ Eq (69), m	0.080	0.083	0.0785	0.082
$L_{measured}$, m	0.202	0.210	0.205	0.204
$L_{calc.}$ Eq (67), m	0.198	0.2054	0.1943	0.203
$F_{b\ experimt.}$, N	1.1564	1.2300	1.1564	1.176
$F_{b\ calc.}$ Eq (68), N	1.1226	1.1647	1.1015	1.1506
F_T, N	1.2936	1.6954	1.9992	3.8024
F_{cb}, N	0.1372	0.4655	0.8428	2.6264

fluid: Methocel K15 MS 2%; θ: 25 (°C); γ_1: 1005 (kg/m^3); a: $1.357 \cdot 10^{-2}$ (m); R: $1.758 \cdot 10^{-2}$ (m); K: 0.772 (-).

Table 3. Values of s = 1/n for experiments A, B, C, D.

$\frac{EXP(i)}{EXP(j)}$*	$\frac{EXP(D)}{EXP(A)}$	$\frac{EXP(D)}{EXP(B)}$	$\frac{EXP(D)}{EXP(C)}$	$\frac{EXP(C)}{EXP(A)}$	$\frac{EXP(B)}{EXP(A)}$
S	1.4398	1.4201	1.548	1.3726	1.4689

$\bar{s}$ = 1.449 and $\bar{n}$ = 0.6897

*s found using data from experiments i and j as required by Equation (80)

Table 4. Values of λ_+, T_w, $\left(\frac{d\phi}{d\rho}\right)_{\rho=K}$ and Φ for n = 0.6897, K = 0.772 and T_o = 0.

Parameter	λ_+	T_w	$\left(\frac{d\phi}{d\rho}\right)_{\rho=K}$	Φ
Value	0.8914	0.257283	0.1397	1203.76.10-6

procedure described in 4.2.4, with K = 0.772 and To = 0, and they are shown in Table 4. Following the procedure described in 4.2.4 the values of pressure drop per unit of length (P), consistency coefficient (η), shear rate at the plunger wall ($(\frac{dv}{dr})_{r=a}$), and shear stress at the plunger wall (τ_w) were also obtained and are presented in Table 5 for experiments A, B, C and D. To experimentally validate the mathematical model, the Methocel solution was used as a model for a power law fluid. Experiments were conducted with a Haake viscometer to determine the rheological properties of the Methocel solution. These values were compared to those value obtained using the extrusion technique.

Table 6 shows the values of the flow behavior index (n) and the consistency coefficient (η) obtained with different sensors on the Haake viscometer. Prior to each experiment, tests were conducted to investigate the possibility of time-dependent phenomenon for this fluid. Methocel solutions did not present time-dependence when tested at 120 rpm using the MV cup and the paddle (impeller) sensor.

For the sensors used in the Haake viscometer, Table 6 shows that the flow behavior index (n) increases as the gap, between the rotor of the sensor wall and the inner cup wall, increases; the same fact occurs with the consistency coefficient (η) values. The order of increasing gap values is MV-I, MV-II, MV-III and SV-I sensor with MV cup used with all the sensors. The differences obtained with the above sensors could be attributed to the presence of wall effects.

Table 5. Values of P, η, $\left(\frac{dv}{dr}\right)_{r=a}$ and τ_w for experiments A, B, C and D

	EXPERIMENT			
	A	B	C	D
P, $[\frac{Pa}{m}]$	880.465	2873.49	5329.42	16689.38
η, [Pa s^n]	2.664	2.8653	3.2947	3.40
$\left(\frac{dv}{dr}\right)_{r=a}$, $[s^{-1}]$	0.656	3.279	6.557	32.788
τ_w, [Pa]	1.99	6.499	12.05	37.746

$$\eta_{average} = 3.056\ [Pa\ s^{0.6897}]$$

The rheological equation is

$$\tau = 3.056\left(\frac{dv}{dr}\right)^{0.6897}$$

Table 6. Rheological values obtained for Methocel K15MS 2% sample using the Haake viscometer and back extrusion.

	Haake Values, 20°C					
	MV-I	MV-II	MV-III	SV-I sensor MV cup	Paddle	Back Extrusion Technique 25°C
n,(-)	0.6081	0.6558	0.6982	0.7049	0.683	0.6897
n,(Pa s^n)	3.654	3.7144	3.810	4.407	3.45	3.056

The MV paddle was used in order to eliminate this possible wall effects. The MV paddle was used in order to eliminate this possible wall effects. Rheological properties for Methocel solution obtained with the MV paddle are also presented in Table 6; the value of n obtained with the MV paddle is close to the value obtained with the MV-III sensor. The value of η was the lowest for the MV paddle, suggesting that some settling occurred as the gap increased in value when using the other sensors.

Also shown in Table 6 are the values of n and η obtained with the back extrusion technique. The value of the flow behavior index (n) obtained with this technique was 0.6897, and it can be seen that it is very close to the value obtained with the MV paddle sensor (n = 0.683). The value is also closed to that obtained with the MV-III sensor (0.6982).

The value obtained for the consistency coefficient (η) with the back extrusion technique is lower than that obtained with the MV paddle sensor; however, the fact that the temperature during the back extrusion test was 25^{o}C and the temperature for MV paddle test was 20^{o}C may explain this difference. The consistency coefficient is known to be strongly dependent on temperature--Arrhenius relationship--and decreases with increasing temperature. The flow behavior index (n) is practically independent of temperature. Based on the results shown in Table 6, it is possible to conclude that the back extrusion technique is a

valid tool for studying the rheological properties of power law fluids.

5.2 Herschel-Bulkley Fluids

When using Kelset solution as Herschel-Bulkley fluids, the force versus distance diagrams obtained in the chart recorder were straight lines that, when extrapolated to zero, gave a positive value of force-force due to the existence of a yield stress in the fluid--as shown in Figure 14.

To obtain the rheological properties of Kelset solutions, the samples were tested for time-dependence by agitating them using the MV paddle run at 20 rpm and 120 rpm while measuring torque decay over time. Time-dependent behavior was not found and consistency coefficient (η) and flow behavior index (n) were evaluated with MV paddle sensor data. Table 7 shows the shear stress (τ) and shear rate ($\frac{dv}{dr}$) values obtained using the power law model. The values of η and n, with the correlation coefficient for n, are shown in Table 8. A Herschel-Bulkley model was fitted to the data shown in Table 7. The values of yield stress (τ_y), consistency coefficient (η) and flow behavior index (n), with the correlation coefficient obtained, are given in Table 9. To fit the data to the Herschel-Bulkley model, the values of τ and ($\frac{dv}{dr}$) corresponding to ($\frac{dv}{dr}$) greater than 10 s^{-1} were considered. From Table 9 it can be seen that the Herschel-Bulkley model gives good agreement with the data shown in Table 7.

Table 7. Shear stress-shear rate values for 2% Kelset solution using mixer viscometry technique .

τ (Pa)	$\frac{dv}{dr}$ (s^{-1})
52.45	2.0
69.40	4.0
81.75	6.0
91.83	8.0
100.49	10.0
108.17	12.0
115.12	14.0
121.50	16.0
127.42	18.0
132.97	20.0
156.63	30.0
166.7	35.0
175.94	40.0
184.5	45.0
192.5	50.0
200.0	55.0
207.25	60.0

Table 8. Rheological properties of 2% Kelset solution using the power law model.

η (Pa s^n)	n (-)	correlation coefficient (-)
39.639	0.4040	0.996

Table 9. Rheological properties of 2% Kelset solution using the Herschel-Bulkley model.

τ_y (Pa)	η (Pa s^n)	n (-)	correlation coefficient (-)
25.17	24.658	0.4901	0.9996

The same Kelset solution, from which a sample was used to obtain its rheological properties with the MV paddle, was used to conduct experiments with the back-extrusion device. Special care was necessary when filling the cylinder with the sample to avoid the presence of air bubbles in the sample.

Table 10 shows the values obtained for a Kelset solution with the back extrusion device, at three different plunger velocities. The values of L, F_b, $\overline{OB}$ and τ_y were calculated using Equations (67), (68), (69) and (76) respectively. The chart speed was set before conducting the experiments and values of l_{ch}, F_{Te} and F_T were obtained from the chart recorder upon completion of testing. From the data shown in Table 10, the values of force corrected for buoyancy (F_{cb}) were calculated using Equation (71). Then, expressions for $\frac{F_{cb}}{\pi LRa}$ were calculated for each velocity used in the test (Table 11).

A computer program was developed to calculate the following: pressure drop per unit of length (P), dimensionless shear stress at the wall (T_w), dimensionless yield stress (T_o) and dimensionless volumetric flow (Φ), when the rheological properties of a fluid are known. The calculations were done for different plunger velocities using the value of K = 0.772 for the dimensionless radius of the plunger. Table 12 shows the result of these calculations for the rheological properties of Kelset given in Table 9.

Table 10. Experimental valves obtained for a Herschel-Bulkley fluid.

	EXPERIMENT				
	E	F	G	H	I
v_p, m/s	$3.33 \cdot 10^{-4}$	$3.33 \cdot 10^{-4}$	$8.33 \cdot 10^{-4}$	$8.33 \cdot 10^{-4}$	$16.667 \cdot 10^{-4}$
C_{sp}, m/s	$50.0 \cdot 10^{-4}$	$50.0 \cdot 10^{-4}$	$50.0 \cdot 10^{-4}$	$50.0 \cdot 10^{-4}$	$50.0 \cdot 10^{-4}$
l_{ch}, m	1.194	1.020	0.559	0.492	0.1677
$\overline{OB}$, m	0.0796	0.068	0.093	0.082	0.0556
L, m	0.1970	0.1683	0.2306	0.2030	0.1380
F_{T_e}, N	1.5974	1.3622	1.813	1.568	1.078
F_b, N	1.138	0.972	1.332	1.172	0.796
F_T, N	4.900	4.116	7.232	6.546	5.537
τ_y, Pa	27.34	27.17	24.46	22.86	24.01

fluid: Kelset 2%; $\gamma_1 = 1018.9$ (Kg/m^3); $a = 1.357 \cdot 10^{-2}$ (m); $R = 1.758 \cdot 10^{-2}$ (m);
$\tau_{y\ average} = 25.17$ (Pa)

Table 11. Values of the expression for $\frac{F_{cb}}{\pi LRa}$ experiments E, F, G, H and I.

Experiment	v_p	$\frac{F_{cb}}{\pi LRa}$
	$\left(\frac{m}{s}\right)$	$\left(\frac{Pa}{m}\right)$
E	$3.33\ 10^{-4}$	25477.0
F	$3.33\ 10^{-4}$	24924.26
G	$8.33\ 10^{-4}$	34140.79
H	$8.33\ 10^{-4}$	35329.59
I	$16.667\ 10^{-4}$	45907.25

Table 12. Values of P, T_w, T_o, $\frac{F_{cb}}{\pi LRa}$ and Φ at different velocities for the rheological properties of Kelset shown in Table 9.

v_p	P	T_w	T_o	$\frac{F_{cb}}{\pi LRa}$	Φ
$\frac{m}{s}$	$\frac{Pa}{m}$	(-)	(-)	$\frac{Pa}{m}$	(-)
$3.33 \cdot 10^{-4}$	29571.3	0.2445	0.097	30059.23	$92.4 \cdot 10^{-6}$
$8.33 \cdot 10^{-4}$	37701.16	0.2466	0.076	38402.4	$140.78 \cdot 10^{-6}$
$16.667 \cdot 10^{-4}$	46658.6	0.248	0.061	47591.77	$182.26 \cdot 10^{-6}$

The procedure described in section 4.2.6 was used to determine the rheological properties of a Herschel-Bulkley fluid in a back extrusion device. Three plunger velocities were used to generate Figure 16. Also, the expressions $\frac{F_{cb}}{\pi LRa}$ obtained from experiments at three plunger velocities and the expressions $\frac{F_{cb}}{\pi LRa}$, obtained in Table 12, are plotted.

The experimental results obtained with a Herschel-Bulkley fluid in a back extrusion device indicate that this is an easy and reliable technique to determine yield stress. It can be concluded that, if a time-independent fluid is of a Herschel-Bulkley type, then its rheological properties can be determined using the back extrusion technique with the mathematical model developed in this study. The differences between the theoretical and experimental values of the expression $\frac{F_{cb}}{\pi LRa}$-which is equal to $P(T_w + K)$--are discussed in the next section.

5.3 Experimental Problems

With the equipment used in this study, there are restrictions, due to the sensitivity of the loading cell used, to determine rheological properties of fluid with low values of apparent viscosity. The speed of response of the instrument is also critical in obtaining accurate force measurements. In further experiments a data acquisition system should be used to collect the data. Also, the instrument should have a device to filter external signals that produce a marked noise in the force-distance diagram.

Another important source of error found during the

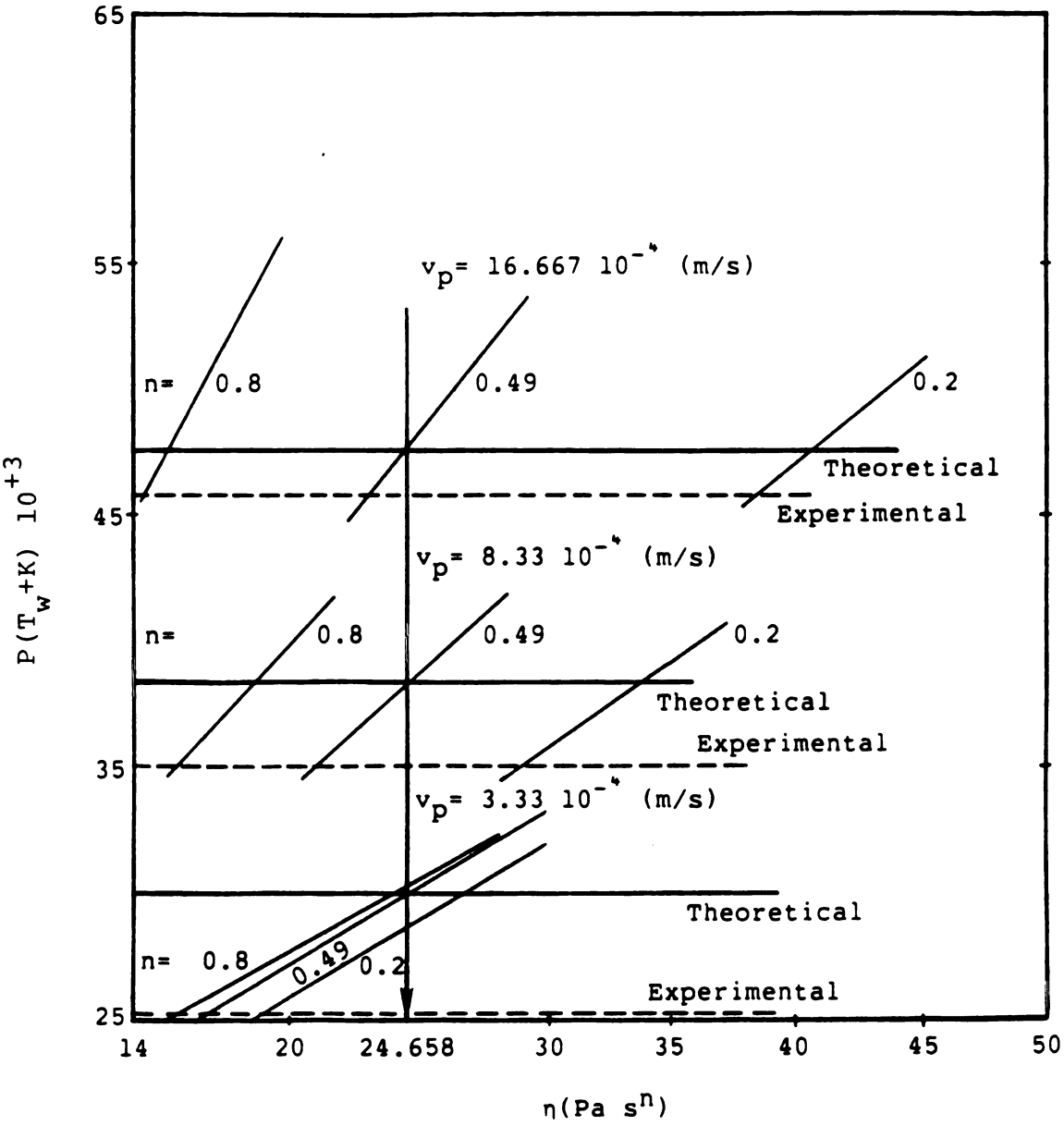

Figure 16. Determination of the rheological properties of a Herschel-Bulkley fluid using the back-extrusion technique.

experiments was the alignment between the cylinder containing the sample and the plunger rod. If the plunger has a small inclination, the fluid flowing upward will have axial and radial velocity components, which would contradict one of the assumptions used to develop the mathematical model.

To eliminate end effects due to the flat-bottom plunger, a pointed or a semi-spherical end could be used. This would reduce separation of the fluid around the end of the plunger; but, on the other hand, it would increase the force due to shear stress, and it would be necessary to calculate this contribution to the total force.

Chapter 6

Conclusions

The conclusions of this study are:

1. It is possible to develop mathematical expressions to describe the behavior of non-Newtonian fluids in a back extrusion device using the Herschel-Bulkley fluid model.
2. The mathematical expressions obtained can be expressed in form of dimensionless terms.
3. It is possible to use graphics and tables, with the dimensionless terms, to facilitate the handling of the mathematical expressions.
4. With the mathematical model developed it is possible to determine the rheological properties of Newtonian, power law, Bingham plastic, and Herschel-Bulkley fluids.
5. With the methods developed in this study, it is possible to determine the shear stress at the plunger wall and the shear rate at the plunger wall at which the rheological properties are obtained.

BIBLIOGRAPHY

BIBLIOGRAPHY

Ashare, E., Bird, R.B., and Lescarboura, J.A. 1965. Falling cylinder viscometer for non-Newtonian fluids. AIChE Journal 11(5):911.

Bird, R.B., Stewart, W.E., and Lightfoot, E.N. 1960. "Transport Phenomena," John Wiley and Sons, Inc., New York, NY.

Bird, R.B. 1965. Experimental tests of generalized Newtonian models containing a zero-shear viscosity and a characteristic time. Can. J. Chem. Eng. 43:161.

Bikerman, J.J. 1948. A penetroviscometer for very viscous liquids. J. Colloid Sci. 3:75.

Cheng, D.C.-H. 1970. A design procedure for pipeline flow of non-Newtonian dispersed systems. In "Proceedings of the First International Conference on the Hydraulic Transport of Solids in Pipes (Hydrotransport 1)," Sept. 1-4. British Hydromechanics Research Association, Cranfield, Bedford, England.

Cheng, D.C.-H. 1975. Pipeline design for non-Newtonian fluids. The Chem. Eng. (London). 301:525; 302:587.

Cramer, S.D., and Marchello, J.M. 1969. Design procedure for laminar, isothermal, non-Newtonian flow in pipes and annuli. Ind. Eng. Chem. Process Des. Dev. 8(3):293.

Ferry, J.D. 1970. "Viscoelastic Properties of Polymers." Second ed. John Wiley and Sons, Inc., New York, NY.

Ford, E.W., and Steffe, J.F. 1984. Rheological properties of starch-thickened fruit puree. Paper No. 84-6007. American Society of Agricultural Engineers. St. Joseph, MI.

Fredrickson, A.G., and Bird, R.B. 1958. Non-Newtonian flow in annuli. Ind. Eng. Chem. 50(3):347.

Fredrickson, A.G. 1959. Flow of non-Newtonian fluids in annuli. Ph.D. Thesis, Univ. Wisconsin.

Hanks, R.W. and Ricks, B.L. 1974. Laminar-turbulent transition in flow of pseudoplastic fluids with yield stresses. J. Hydronautic 8(4):163.

Hanks, R.W. 1978. Low Reynolds number turbulent pipeline flow of pseudo-homogenous slurries. In "Proceedings of the Fifth International Conference on the Hydraulic Transport of Solids in Pipes (Hydrotransport 5 paper C2)," May 8-11. British Hydromechanics Research Association, Cranfield, England.

Hanks, R.W. and Larsen, K.M. 1979. The flow of power law non-Newtonian fluids in concentric annuli. Ind. Eng. Chem. Fundam. 18(1):33.

Hanks, R.W. 1979. The axial laminar flow of yield-pseudoplastic fluids in a concentric annulus. Ind. Eng. Chem. Proces des. Dev. 18(3):488.

Harper, J.P., Suter, D.A., Dill, C.W. and Jones, E.R. 1978. Effets of heat treatment and protein concentration on the rheology of bovine plasma protein suspensions. J. Food Sci. 43:1204.

Herschel, W.H. and Bulkley, R. 1926. Konsistenzmessungen von gummi-benzoltosunge. Kolloid-Z. 39:291.

Laird, W.M. 1957. Slurry and suspension transport. Ind. Eng. Chem. 49(1):138.

McEachern, D.W. 1966. Axial laminar flow of a non-Newtonian fluid in an annulus. AIChE Journal. 12(2):328.

Melrose, J.C., Savins, J.G., Foster,W.R., and Parish, E.R. 1958. A practical utilization of the theory of Bingham platic flow in stationary pipes and annuli. Pet. Trans. AIME. 213:316.

Morgan, R.G., Suter, D.A., and Sweat, V.E. 1979. Mathematical analysis of a simple back-extrusion device. Paper No. 79-6001. American Society of Agricultural Engineers. St. Joseph, MI.

Philippoff, W. 1965. Relaxations in polymer solutions, liquids and gels. In: "PHysical acoustics," vol. 2B, Academic Press, New York, NY.

Rotem, Z., and Shinnar, R. 1961. Non-Newtonian flow between parallel boundaries in linear movement. Chem. ENg. Sci. 15:130.

Rotem, Z. 1962. Non-Newtonian flow in annuli. J. Applied Mech., Trans. ASME. 29(2):421.

Russell, C.P., and Christiansen, E.B. 1974. Axial, laminar, non-Newtonian flow in annuli. Ind. Eng. Chem. Process Des. Dev. 13(4):391.

Savins, J.G. 1958. Generalized Newtonian (pseudoplastic) flow in stationary pipes and annuli. Pet. Trans. AIME. 213:325.

Skelland, A.H.P. 1967. "Non-Newtonian Flow and Heat Transfer," John Wiley and Sons, Inc., New York.

Paslay, P.R., and Slibar, A. 1957. Laminar flow of drilling mud due to axial pressure gradient and external torque. Pet. Trans. AIME. 210:310.

Smith, T.L., Ferry, J.D., and Schremp, F.W. 1949. Measurements of the mechanical properties of polymer solutions by electromagnetic transducers. J. Appl. Phys. 20:144.

Tiu, C., and Bhattacharyya, S. 1974. Developing and fully developed velocity profiles for inelastics power law fluids in an annulus. AIChE Journal. 20(6):1140.

Van Olphen, H. 1950. Pumpability, rheological properties, and viscometry of drilling fluids. J. Inst. Pet. 36:223.

Vaughn, R.D., and Bergman, P.D. 1966. Laminar flow of non-Newtonian fluids in concentric annuli. Ind. Eng. Chem. Process Des. Dev. 5(1):44.

Whorlow, R.W. 1980. "Rheological Techniques," Halstead Press, New York.